RSC Medicinal Chemistry

ROYAL SOCIETY OF CHEMISTRY

RESEARCH ARTICLE

View Article Online
View Journal | View Issue

Cite this: *RSC Med. Chem.*, 2023, **14**, 2012

Design, synthesis, electrochemistry and anti-trypanosomatid hit/lead identification of nitrofuranylazines†

Maryna Saayman,[a] Christina Kannigadu,[a] Janine Aucamp,[a] Helena D. Janse van Rensburg,[a] Cassiem Joseph,[b] Andrew J. Swarts[b] and David D. N'Da*[a]

Chagas disease and leishmaniasis are vector-borne infectious diseases affecting both humans and animals. These neglected tropical diseases can be fatal if not treated. Hundreds to thousands of new Chagas disease and leishmaniasis cases are being reported by the WHO every year, and currently available treatments are insufficient. Severe adverse effects, impractical administrations and increased pathogen resistance against current clinical treatments underscore a serious need for the development of new drugs to curb these ailments. In search for such drugs, we investigated a series of nitrofuran-based azine derivatives. Herein, we report the design, synthesis, electrochemistry, and biological activity of these derivatives against promastigotes and amastigotes of *Leishmania major*, and *L. donovani* strains, as well as epimastigotes and trypomastigotes of *Trypanosoma cruzi*. Two leishmanicidal early leads and one trypanosomacidal hit with submicromolar activity were uncovered and stand for further *in vivo* investigation in the search for new antitrypanosomatid drugs. Future objective will focus on the identification of involved biological targets with the parasites.

Received 12th May 2023,
Accepted 12th August 2023

DOI: 10.1039/d3md00220a

rsc.li/medchem

Introduction

Neglected tropical diseases (NTDs) consist of several conditions that are prevalent in tropical regions,[1] and can negatively impact individuals through stigmatisation, social rejection, disabilities, discrimination, and financial strain.[2] Leishmaniasis and Chagas disease are both NTDs caused by *Leishmania* and *Trypanosoma* parasites, respectively. These parasites are taxonomically related protozoa that belong to the *Trypanosomatidae* family (order *Kinetoplastida*) and accordingly have similar biochemical and structural features.[3]

Leishmaniasis is transmitted to humans during hematophagy of infected female *Phlebotomus* sandflies.[4] There are over twenty *Leishmania* species that can affect humans and three clinical forms in which leishmaniasis can occur.[5] These forms are cutaneous (CL), which can be identified by lesions on the skin; mucocutaneous (MCL), a differentiated form with lesions on the mouth and skin; and visceral leishmaniasis (VL), identified by skin lesions and a systemic infection that results in an immune deficiency.[6] CL mainly occur in the Americas, Middle East, Mediterranean basin, and Central Asia, while VL is more prevalent in Brazil, India, and East Africa, and MCL in Brazil, Peru, and Ethiopia.[7] In 2021, there were 221 731 new CL[8] and 11 450 new VL[9] cases reported by the World Health Organization (WHO); however, it is estimated that only 25 to 45% of VL cases are being reported, therefore making the annual occurrence 50 000 to 90 000 cases.[7] VL is fatal when left untreated, while MCL can also be fatal when secondary complications occur.[10]

Chagas disease (American trypanosomiasis), on the other hand, is mainly transmitted to humans through contact with the urine and/or faeces of blood-sucking triatomine insects infected with *T. cruzi* parasites.[11] It can also be transmitted through blood transfusions, congenital transmission, organ transplants, and laboratory accidents.[12] This disease presents in two clinical phases, acute and chronic. The acute phase, lasting approximately 2 to 4 months, is usually asymptomatic. The chronic phase, which can last decades after infection, can either be asymptomatic or symptomatic.[13] Symptoms of active chronic infection include chronic gastrointestinal disease and/or heart disease with low, fluctuating parasitaemia levels.[14] Approximately 6 to 7 million individuals worldwide are infected with the *T. cruzi* parasite, with an annual occurrence of about 30 000 new

[a] *Centre of Excellence for Pharmaceutical Sciences, North-West University, Potchefstroom 2520, South Africa. E-mail: David.Nda@nwu.ac.za; Fax: +27 18 299 4243; Tel: +27 18 299 2256*
[b] *Molecular Sciences Institute, School of Chemistry, University of the Witwatersrand, Johannesburg-Braamfontein 2050, South Africa*
† Electronic supplementary information (ESI) available. See DOI: https://doi.org/10.1039/d3md00220a

cases, 12 000 deaths, and 8600 infants infected during gestation by the Pan American Health Organization (PAHO), a specialised agency of the United Nations (UN) in charge of international health cooperation in the Americas.[15] Chagas disease is mostly found in endemic Latin American countries.[11]

There are no vaccines for protection against both infections; however, chemotherapeutic drugs are available for the treatment of leishmaniasis and Chagas disease. Leishmaniasis treatment consists of pentavalent antimonies (sodium stibogluconate and meglumine antimonate), amphotericin B, paromomycin, miltefosine, pentamidine and the azoles (ketoconazole, itraconazole and fluconazole).[16–18] These drugs have several limitations, such as impractical administration, toxicity, steep cost, and parasite resistance.[19] The fight against the latter is an ongoing battle due to the misuse of drugs, financial constraints, and the unavailability of new drugs.[20]

The treatment for Chagas disease consists only of benznidazole or nifurtimox.[21] If administered soon after infection occurs, both medicines are nearly 100% effective in curing the disease. However, the efficacy of the treatment decreases as the disease progresses.[22]

The use of clinical nitrofurans (cNFs) to treat various infectious diseases has been well established over recent years.[23,24] The diverse biological activities of nitrofurans have been attributed to their nitro group and its ability to undergo one-electron transfer reduction, thereby forming reactive oxygen species (ROS) upon Fenton reactions with enzymes.[23,25] Additionally, cNFs (Fig. 1) also have a hydrazone moiety (blue in Fig. 1) that possesses anti-infective activity. The hydrazone moiety also confers diverse biological and pharmacological properties, such as anticancer,[26] antimicrobial,[27] antitrypanosomal,[28] antimycobacterial,[29] anticonvulsive,[30] anti-inflammatory[31] and analgesic properties.[32] Altogether, these pharmacological features enhance the stand of cNFs as potentially repurposable drugs for the treatment of infectious diseases such as leishmaniasis and Chagas disease.

Research literature indicates that azines consisting of a C=N–N=C functional unit (Fig. 2) possess bactericidal and antiparasitic properties.[33] These compounds are highly basic and form salts very easily, thus they are endowed with increased water solubility and become equivalent to hydrazones in the protonated state. They are also thermally

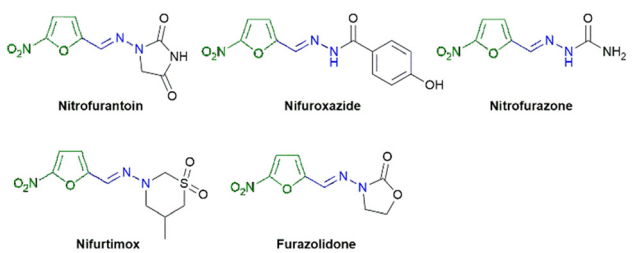

Fig. 1 Clinical nitrofuran drugs.

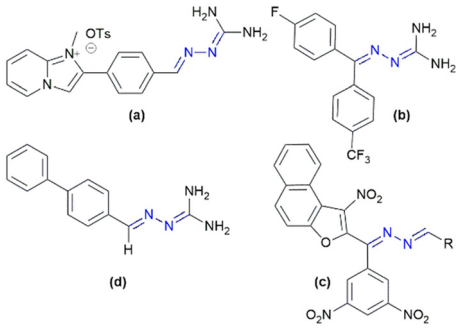

Fig. 2 Structures of biologically active azines with: (a) trypanocidal, (b) antimalarial, (c) and (d) antibacterial agents.

and chemically more stable than their hydrazone tautomers.[33,34] The azine bridge acts as electronic effect communicator between the substituents on its terminal imine carbon atoms.[35]

Moreover, the use of aromatic rings in drug design is a well-known strategy as they offer numerous unique and strong interaction modes with target proteins, which include classical arene–arene (π-stacking) interactions, as well as arene–H bonding (edge-to-face interactions), and other interactions, such as sulphur–arene interactions.[36] Thus, the linking of nitrofuran, azines and aromatic rings may result in compounds that are more biologically active and stable.

Based on these previous findings, nitrofuran-based azine derivatives and their antiprotozoan activities were examined *in vitro*. We herein present the synthesis and the biological activities of these nitrofuranylazines.

Results and discussion

Chemistry

Nitrofuran-based azine derivatives (**1a–9a**, **1b–9b**) were synthesised *via* a two-step process depicted in Scheme 1, starting from commercially available 5-nitro-2-furaldehyde (NFA) or 5-nitrothiophene-2-carboxaldehyde (NTA). Firstly, the hydrazone intermediates **1–9** were prepared by reacting various substituted aldehydes with excess hydrazine hydrate (6-fold equivalent), which was needed to prevent the early formation of unwanted symmetrical arylazines and were isolated after recrystallisation from ethyl acetate. This was then followed by a Schiff base reaction of intermediates with NFA or NTA to afford the targeted nitrofuran-based azine derivatives (**1a–9a**, **1b–9b**) in poor to excellent yields of 13–98% after purification by recrystallisation from ethyl acetate or column chromatography. The poor yields were attributed mainly the poor rate of reaction and purification process. For example, the synthesis of **5a**, **8a** and **7b** was unsuccessful in the acidic medium, hence a basic medium with the addition of potassium carbonate was used. Yet, after 48 hours, considerable amounts of unreacted reagents were still present in the reaction mixture. No optimisation was attempted, which may be a future endeavour especially if

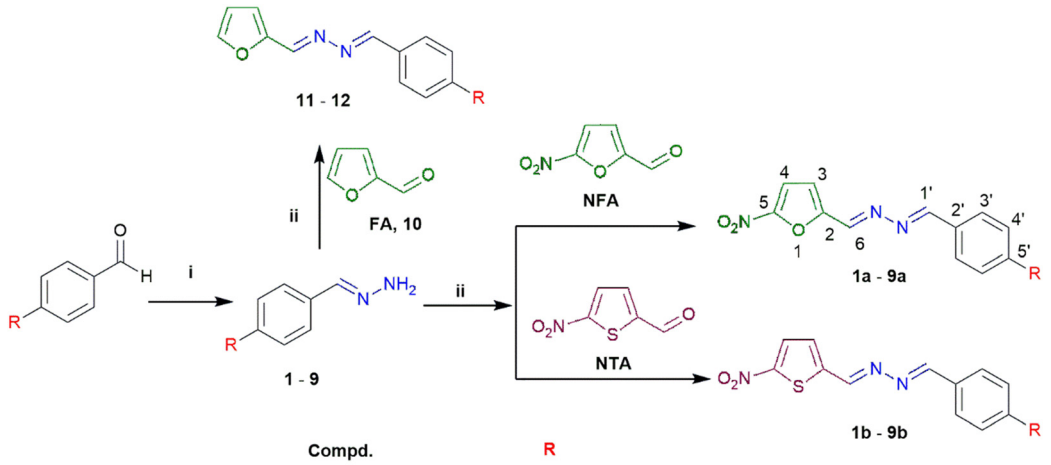

Compd.	R
1 (47%); **1a** (47%), **1b** (27%)	H
2 (62%); **2a** (66%); **2b** (55%)	F
3 (65%); **3a** (60%); **3b** (27%)	Cl
4 (61%); **4a** (78%); **4b** (41%)	Br
5 (85%); **5a** (13%); **5b** (24%)	Me
6 (67%); **6a** (27%); **6b** (46%)	OMe
7 (84%); **7a** (75%); **7b** (13%)	OBn
8 (71%); **8a** (14%); **8b** (42%)	OH
9 (91%); **9a** (62%); **9b** (66%)	NO_2
11 (29%)	OBn
12 (61%)	NO_2

Scheme 1 Two-step synthesis of target nitrofuranylazines. Reagents and conditions: i. hydrazine hydrate (6 equiv.), TEA (1.5 equiv.), EtOH (10 mL), rt, 12 h; ii. NFA/NTA/FA (1 equiv.), EtOH (10 mL), rt, 12 h.

these poorly yielded azines happen to be among the most biologically active of compounds of this investigation.

The aldazines were divided into two chalcogen series, nitrofuran (oxygen chalcogen, series A) and nitrothiophene (sulphur chalcogen, series B).

Furthermore, to validate nitrofuran as pharmacophore of the azines, furfural was reacted with selected hydrazone intermediates, namely **7** and **9**, which resulted in azines **11** and **12**, omitting the nitro group. The characterisation spectra of all synthesised compounds are provided as ESI† (Appendix A).

The formation of the hydrazone intermediates (**1**–**9**) was illustrated *via* ^{1}H NMR through the disappearance of the characteristic aldehyde proton at *ca.* δ 10.0 ppm and the appearance of a previously absent singlet at δ 7.65 ppm, indicative of the imine proton of the newly formed hydrazone bond C*H*═NH–NH_2. This was further corroborated by the appearance of the characteristic singlet at *ca.* δ 6.60, representative of the terminal primary amine protons N*H*$_2$. The disappearance of this NH_2 peak from the spectra of **1a**–**9a** and **1b**–**9b** confirmed the success of the Schiff base reaction. This was further verified by the appearance of two separate vinylic protons H-1′ and H-6 of the azine bond as characteristic singlets at *ca.* δ 8.79 and 8.65 ppm.

The fluorine-containing azines (*i.e.*, **2a**, **2b**) exhibited proton-fluorine coupling, and it was found that the protons of interest, H-3′ and H-4′, underwent mostly *ortho* couplings with J_{H-F} ~ 8–9 Hz. Through careful examination of all the ^{1}H spectra, it was determined that all the protons of each azine were accounted for.

The ^{13}C spectra of the aldazines showed the two hydrazone moiety peaks of C-1′ at δ 162.7 and C-6 at δ 149.8. Carbon–fluorine coupling (J_{C-F}) also occurred in compounds **2a** and **2b** which exhibited J values of *ca.* $^1J_{C\text{-}5'\text{–}F}$ = 250 Hz, $^2J_{C\text{-}3'\text{–}F}$ = 9.0 Hz, $^3J_{C\text{-}3'\text{–}F}$ = 3.0 Hz and $^4J_{C\text{-}2'\text{–}F}$ = 22.0 Hz.

IR spectroscopy further confirmed the success of the Schiff base reactions through the appearance of characteristic stretching absorptions: C═N (1600–1560 cm^{-1}) and N–O (1550–1500 and 1350–1300 cm^{-1}). The HRMS using atmospheric pressure chemical ionisation (APCI) source confirmed the integrity of the synthesised aldazines as in all cases, the molecular ions corroborated the proposed structures.

Of note, azines may occur in three configurational isomers, *i.e.* (*E*,*E*), (*E*,*Z*), and (*Z*,*Z*).[37,38] Photochemical isomerisation of C═N bonds can result in the production of isomers (*E*,*Z*) and (*Z*,*Z*) from (*E*,*E*), which is thermodynamically the most stable form.[39] A sequence of four atoms (C═N–N═C) determines the configuration of aromatic azines. X-ray diffraction (XRD) studies indicate that mostly all of reported aromatic azines exhibit the preferred (*E*,*E*) configuration where

large groups linked to the imine carbons (*C*═N–) are *trans* to the N–N bond, due to reduced repulsive interactions with the lone pair of the N atoms.[40] The current azines were not subjected to XRD analysis, and to the best of knowledge, they are novel. However, XRD studies of ferrocenylazines bearing the 5-nitrofuran and 5-nitrothiophene scaffolds have previously been conducted by Gómez *et al.*[35,41] and confirmed the (*E*,*E*) configuration of these aromatic azines. In this configuration, the ^{1}H chemical shifts (δ) of the azine bridge protons were found to be in the 8.38–8.36 ppm region, wherein those of protons H-6 and H-1′ of the current azines also fell. Accordingly, the (*E*,*E*)-configuration was presumed for all the aldazines in this study.

In silico physicochemical and pharmacokinetic properties

The physicochemical and pharmacokinetic properties of the synthesised compounds and standard nitrofuran drugs were determined using the SwissADME web tool and presented in ESI† (Appendix B).

The $\log P_{o/w}$ value of a molecule is the partition coefficient between octanol (lipophilic phase) and water (hydrophilic phase).[42] $\log P_{o/w}$ is used to examine important biological properties for drug action, which include lipid solubility, distribution in tissue, binding to receptors, cellular uptake, metabolism, and drug bioavailability.[43] According to Lipinski *et al.*,[44] $\log P_{o/w}$ values are targeted in the 1–5 range, with 1–3 being ideal for orally deliverable drugs. All the synthesised compounds presented with a $\log P_{o/w}$ of 1–5, whereas the parent drugs, NFA and NTA, and reference antibiotics, NFX, FZD, NFZ and NFT, fell below 1 due to their higher hydrophilic affinities. This in theory implies an overall improvement in oral bioavailability.

Furthermore, all synthesised azines complied with Lipinski's rules and had physicochemical properties well within the target ranges.[44] Lipophilicity, although a crucial physiochemical parameter, is not the only determining characteristic of good drug design, as evident by other successful drugs that do not fall within the target range.[45] Therefore, other drug parameters, such as topological polar surface area (TPSA), were predicted for these compounds. TPSA is the surface area of a molecule that emerges from nitrogen or oxygen atoms, as well as hydrogen atoms that are attached to oxygen or nitrogen atoms.[46] TPSA shows the correlation with passive molecular transport through membranes, which allows the prediction of gastrointestinal (GI) absorption, Caco-2 monolayer permeability, and penetration of the blood–brain barrier. All the derivatives, apart from **9b**, were predicted to be highly absorbed in the gastrointestinal (GI) tract through passive diffusion and were, therefore, expected to be druglike by nature (ESI† table). This also indicates that the possible mode of delivery for these azine analogues would be oral administration, except for **9b**, which will possibly be intravenous or intramuscular administration.

Electrochemistry

The biological activity of nitroheterocyclic compounds results from their capacity to undergo oxidation–reduction process by one electron-transfer and their selective toxicity is determined by reduction to the biologically active form in the absence of oxygen.[47–49] Hence, electrochemical testing was used to assess the redox properties of the synthesised aldazines. Cyclic voltammetric experiments determined their half redox potentials ($E_{1/2}$) at room temperature using a scan rate of 100 mV s^{-1} and solution of 0.5 mM in anhydrous acetonitrile (MeCN), with 0.1 M [^{t}BuN][PF_6] as the background electrode. The redox potentials were measured using glassy carbon, Pt wire and Ag/AgCl as the working, counter, and reference electrodes, respectively. The data are summarised in Table 1.

The voltammograms of all azines displayed reversible waves with $E_{1/2}$ values in the −0.96 to −0.85 V range, as shown in Fig. 3 for azine **7a**, when scanned over the range of −1.7 to +1.0 V.

Comparing the reduction waves (E_{pc}) and i_{pa}/i_{pc} ratios, all azines **1a–9a** and **1b–9b** had values of −1.0 to −1.08 V, and *ca.* 1, respectively, which are indicative of a reversible-controlled one-electron transfer process that was attributed to the reduction of the Ar–NO_2 to form a stable anion radical (*i.e.*, Ar–$NO_2^{\bullet-}$) as previously reported.[35] However, all azines possessed negative $E_{1/2}$ values which may also suggest that their nitroaromatic groups are less readily reduced. The $E_{1/2}$ value of nitrofuran clinical trypanocidal drug, NTX, is −0.88 V, as reported by Gómez *et al.*[35] Compounds NFA, **1a** and **2b** presented with $E_{1/2}$ values comparable to that of NTX, whereas **6a** and **3b** were only slightly lower (−0.85 V). Since *Leishmania* and *Trypanosoma* are taxonomic kinetoplastid parasites, these aldazines and nifurtimox may display comparable trypanocidal and leishmanicidal potencies, which may be more pronounced for NFA and **1a** as these two compounds have the same $E_{1/2}$ value of −0.88 V as NTX. The remaining majority had higher half-potentials ($E_{1/2} \geq 0.9$ V), which could suggest a tendency to be less reduced than NTX. As the general biological activity and selective toxicity of nitroheterocyclic compounds depend on their capacity to undergo oxidation–reduction *via* electron-transfer and anaerobic reduction, respectively, this may indicate reduced activity compared to NTX.

Further scrutiny of the data revealed that, in reference to NFA, the reduction potential ($E_{1/2}$) of its derived azines, **2a–9a**, show a slight cathodic shift which suggests that these azines are more readily reduced (though marginally) than the parent NFA due to the incorporation of more electron-donating groups. This assertion is corroborated by aldazines **5a**, **6a**, **7a** and **8a** that contain the electron-donating groups (EDGs), methyl (Me), MeO (methoxy in *para*-position), benzyloxy (BnO) and hydroxy (OH), respectively on the phenyl

Table 1 Electrochemical data of nitroaromatic azines[a]

Compd.	Nitroaromatic redox group	Redox potentials				
		E_{pa}[b] (V)	E_{pc}[c] (V)	$E_{1/2}$[d] (V)	ΔE_p[e] (V)	i_{pa}/i_{pc}[f]
NFA	NO_2–NF	−0.74	−1.02	−0.88	0.28	0.967
1a	NO_2–NF	−0.76	−1.00	−0.88	0.24	1.016
2a	NO_2–NF	−0.78	−1.06	−0.92	0.28	0.990
3a	NO_2–NF	−0.80	−1.08	−0.94	0.28	0.967
4a	NO_2–NF	−0.80	−1.06	−0.93	0.26	0.891
5a	NO_2–NF	−0.82	−1.06	−0.94	0.24	1.007
6a	NO_2–NF	−0.68	−1.02	−0.85	0.34	0.965
7a	NO_2–NF	−0.78	−1.04	−0.91	0.26	1.008
8a	NO_2–NF	−0.82	−1.08	−0.95	0.26	0.943
9a	NO_2–NF & NO_2–Ph	−0.84	−1.06	−0.95	0.22	0.963
NTA	NO_2–NT	−0.86	−1.06	−0.96	0.20	0.755
1b	NO_2–NT	−0.84	−1.06	−0.95	0.22	1.032
2b	NO_2–NT	−0.78	−1.00	−0.89	0.22	1.022
3b	NO_2–NT	−0.74	−0.96	−0.85	0.22	0.889
4b	NO_2–NT	−0.80	−1.04	−0.92	0.24	0.961
5b	NO_2–NT	−0.78	−1.02	−0.90	0.24	1.000
6b	NO_2–NT	−0.80	−1.04	−0.92	0.24	0.990
7b	NO_2–NT	nd	nd	nd	nd	nd
8b	NO_2–NT	−0.82	−1.06	−0.94	0.24	1.002
9b	NO_2–NT & NO_2–Ph	−0.82	−1.06	−0.94	0.24	0.951
NTX	NO_2–NF	nd	nd	−0.88[g]	nd	nd

NFA: 5-nitro-2-furaldehyde; NTA: 5-nitro-2-thiophenecarboxaldehyde; NTX: nifurtimox; NF: nitrofuran; NT: nitrothiophene; Ph: phenyl; nd: not determined. [a] Measured in acetonitrile at a scan rate of 100 mV s^{-1} (V *vs.* Ag/AgCl). [b] Anodic wave potential. [c] Cathodic wave potential. [d] Half wave potential ($E_{1/2} = (E_{pa} + E_{pc})/2$). [e] Wave potential separation ($E_p = E_{pa} - E_{pc}$). [f] Ratio of anodic to cathodic current. [g] Historical data.[35]

(Ph) ring while the remaining azines, **2a**, **3a** and **9a** harbour electron-withdrawing groups (EWGs).

On the contrary, in reference to NTA, the reduction potential ($E_{1/2}$) of the sulphur chalcogen azines **1b**–**9b** showed no discernible differences except for **2b** and **3b**. This could be attributed to both azines bearing EWGs, chlorine and bromine, respectively, while for the remaining azines of the subseries, the electronic nature seemed relatively the same which resulted in their comparable $E_{1/2}$ values.

Fig. 4 shows comparisons of molecular weight, log*P* and electronic effect with electrochemical data of the azines with no obvious correlations found.

Pharmacology

The *Leishmania* parasite presents in two different morphological forms throughout its life cycle; the motile flagellated promastigote form (present in the vector), and the intracellular non-flagellated amastigote form (present in mammalian host cells).[50] *T. cruzi* presents in three different forms throughout their life cycle: the epimastigote form (present in the vector), the trypomastigote form (present in the host), and the amastigote form (present in the host).[51] Of these, the amastigotes are the clinically relevant forms for drug development against *Leishmania* and *T. cruzi* infections, due to their responsibility in the development of the infection and progression to the disease state.[52] However, trypomastigotes of *T. cruzi* are also valuable as a drug target due to them being the infective, non-proliferative blood circulating form, and thus disease progression may be prevented through their death.[53] Nonetheless, it is still beneficial to screen compounds against *in vitro* promastigote and epimastigote forms, along with trypomastigote and amastigote forms, to identify possible antiprotozoal hits.[54] The synthesised derivatives were therefore assessed for their *in vitro* antileishmanial activity against the promastigotes and amastigotes of two *Leishmania* strains, *L. donovani* 9515 and *L. major* IR-173. These *Leishmania* spp. were selected to determine the specificity of the synthesised derivatives against CL- and VL-causing species, *L. major* and *L. donovani*, respectively.[5] The *in vitro* antitrypanosomal activity of the compounds was also assessed against the epimastigotes and trypomastigotes of *T. cruzi* strain, the causative agent of Chagas disease. Amphotericin B (AmB) and benznidazole were used as standard drugs for antileishmanial and antitrypanosomal activity, respectively, alongside the reference cNFs, nifuroxazide, furazolidone, nitrofurazone and nitrofurantoin. The parent compounds, NFA, NTA were also

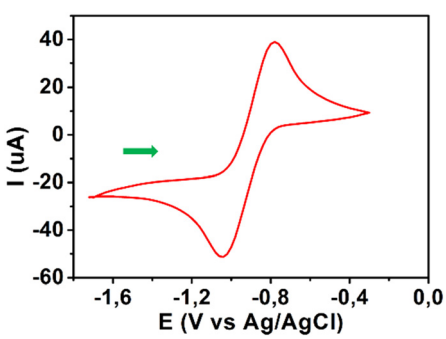

Fig. 3 Cyclic voltammogram of **7a** (0.5 mM) in 0.1 M ^{t}BuNPF$_6$/MeCN recorded at a scan rate of 100 mV s^{-1}.

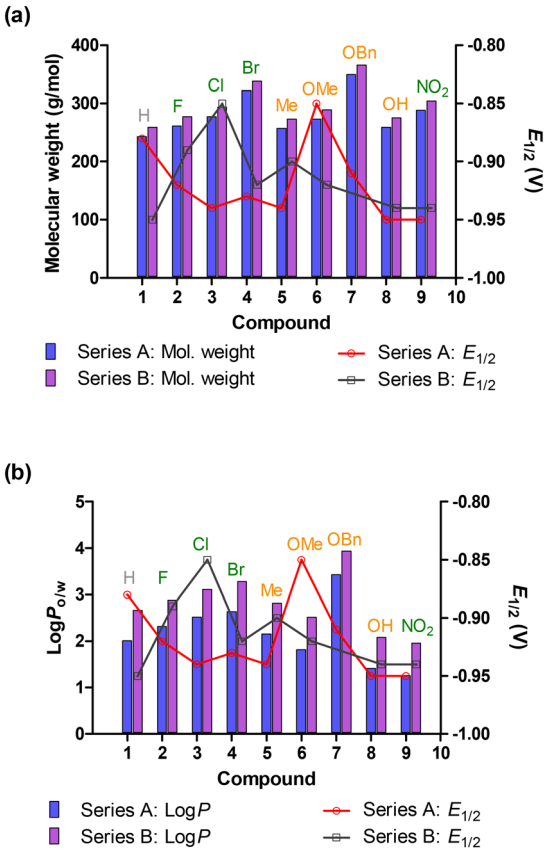

Fig. 4 Comparison of electrochemistry data with electronic effect, (a) molecular weight and (b) *in silico* log *P* data. EWGs are indicated in green, whereas EDGs were indicated in orange and the neutral group was indicated in grey.

screened for comparison. General cytotoxicity profiles of these derivatives were determined using Vero cells with emetine (EM) as a positive control. Specific host macrophage cytotoxicity was assessed using the human leukemia monocytic cell line, THP-1.

All the compounds were initially screened at 10 μM for potential antipromastigote and anti-amastigote activities. Compounds with antipromastigote growth inhibition of >70% qualified for IC_{50} determination,[54] whereas those with anti-amastigote growth inhibition of >60% qualified for IC_{50} determination.[55]

For the anti-amastigote IC_{50} determination, a modified method of Jain *et al.*[56] on parasite rescue and transformation was used. The anti-amastigote activity was measured 72 hours post lysis to detect signs of amastigote recovery and subsequent transformation to and proliferation as promastigotes. Compounds that retained significant antileishmanial activity up to 72 hours post macrophage lysis, indicative of loss in amastigote recovery to proliferative promastigotes, were thus deemed leishmanicidal. The antileishmanial activities and cytotoxicity of the screened compounds are summarised in Tables 2 and 3.

All compounds were also initially screened at 10 μM for potential anti-epimastigote and antitrypomastigote activities. Currently, there are no published cut-off values for these assays. Accordingly, as the epimastigotes are cultured and assayed similarly to *Leishmania* promastigotes, the growth inhibition cut-off of >70% was also applied for the selection of anti-epimastigote compounds for IC_{50} determination. For the trypomastigote screening cut-off, >70% was also applied due to the axenic/host-free nature of the trypomastigote cultures. The antitrypanosomal activities of the screened compounds are summarised in Table 4.

As suggested by the log *P* values hinting towards lipophilic properties, the compounds presented with significantly more solubility problems compared to the reference drugs when solutions were prepared in both 1% DMSO and growth medium, forming quickly separating suspensions that made uniform sampling challenging. This resulted in relatively significant standard deviations for several compounds.

The synthesised intermediates (**1–9**) and several of the azine derivatives exhibited no antiprotozoal activity, thus were not reported in Tables 1–3 as they did not qualify for IC_{50} determination. The cytotoxicity data indicated that nitrofuran derivatives **1a**, **2a**, **6a**, **8a** and **9a** (series A) were moderately toxic to mammalian cells (10 μM < IC_{50} < 50 μM),[57,58] whereas compounds **3a**, **4a**, **5a** and **7a** had low toxicity (IC_{50} > 100 μM).[59,60] The four nitrothiophene chalcogen counterparts that qualified for antiparasitic IC_{50} determination (series B) showed a similar trend, with the **1b** and **8b** presenting with moderate toxicity, whereas **2b** and **7b** had low toxicity toward mammalian cells, inferring that their observed antileishmanial activities were intrinsic. The comparison of cytotoxicity is depicted in Fig. 5.

Comparison of the cytotoxicity with the $E_{1/2}$ values did not show any correlation.

Antileishmanial activity. The nitrofuranyl aldazines exhibited insignificant higher potent activity against both *Leishmania* strains. They were particularly more active against the promastigotes when compared to their nitrothienyl counterparts (**1b–9b**). The comparative activities are shown in Fig. 6.

Nitrofuran aldazines, **2a**, **3a**, **4a** and **9a** presented with cidal anti-amastigote activity against *L. major*. Of these, **2a** and **3a** qualified as antileishmanial hits (IC_{50} < 10 μM; SI > 10).[52] However, azine **9a** presented with moderate to significant cytotoxicity against Vero and host THP1 cells, hence it does not qualify as an antileishmanial hit. The activities of these compounds were comparable to those of NFA and the nitrofuran antibiotic FZD, indicating that the activity of these azines did not improve on that of two references and the standard drug, AmB. However, the cytotoxicity of **2a** and **3a** were less than those of NFA and AmB. The antileishmanial activity of compounds **2a**, **3a** and **9a** were more selectively directed towards the promastigote form (SpI < 0.4).[55] Conversely, nitrofuranylazine **4a** qualified as potential antileishmanial lead (IC_{50} < 1 μM; SI > 100)[52] with specificity towards both parasite forms (0.4 < SpI < 2),[55] significantly improving on the cytotoxicity and antileishmanial activity of the reference drugs against *L. major*.

Table 2 Antileishmanial activities (μM ± standard deviation) of compounds against *L. major* strain IR173

Compd.	General cytotoxicity Vero IC_{50} (μM)	Host cell cytotoxicity THP-1 IC_{50} (μM)	Anti-promastigote activity		Anti-amastigote activity			
			IC_{50} (μM)	SI_1[a]	IC_{50} (μM)	SI_2[b]	SI_3[c]	SpI_1[d]
NFA	17.82 ± 0.25	80.92 ± 6.37	7.94 ± 0.79	2	5.60 ± 0.44	3	14	1.42
1a	16.29 ± 3.50	>100	1.19 ± 0.29	14	>10	—	—	—
2a	47.42 ± 1.12	63.37 ± 5.49	0.73 ± 0.09	65	3.69 ± 0.24	13	17	0.20
3a	>100	>100	0.42 ± 0.07	238	2.47 ± 0.43	40	40	0.17
4a	>100	>100	0.75 ± 0.18	133	0.63 ± 0.02	159	159	1.19
5a	>100	>100	0.42 ± 0.08	238	>10	—	—	—
6a	51.01 ± 1.26	>100	0.89 ± 0.12	57	>10	—	—	—
7a	>100	>100	0.45 ± 0.02	222	>10	—	—	—
8a	18.66 ± 1.31	46.20 ± 5.02	0.64 ± 0.10	29	>10	—	—	—
9a	11.56 ± 1.12	16.75 ± 1.14	0.70 ± 0.10	17	7.90 ± 0.19	1	2	0.09
NTA	12.42 ± 0.88	26.69 ± 0.72	3.75 ± 0.39	3	>10	—	—	—
1b	42.00 ± 8.79	>100	1.43 ± 0.19	29	>10	—	—	—
2b	>100	>100	3.79 ± 0.70	26	>10	—	—	—
7b	>100	>100	4.39 ± 0.24	23	>10	—	—	—
8b	33.12 ± 1.22	22.87 ± 0.13	2.22 ± 0.00	15	>10	—	—	—
11	>100	—	>10		>10			
12	>100	—	>10		>10			
NFZ	>100	>100	1.85 ± 0.06	54	>10	—	—	—
FZD	>100	>100	0.34 ± 0.03	294	5.61 ± 1.89	18	18	0.06
Em	0.08 ± 0.009	—	—	—	—	—		—
Bzn	>100	>100	—	—	—	—		—
AmB	57.80 ± 3.20	14.86 ± 0.09	0.03 ± 0.01	1927	0.47 ± 0.01	123	32	0.06

[a] Selectivity indexes of *L. major*: SI_1 = IC_{50} Vero/IC_{50} promastigote. [b] SI_2 = IC_{50} Vero/IC_{50} amastigote. [c] SI_3 = IC_{50} THP-1/IC_{50} amastigote. Specificity index (SpI) < 0.4 indicates more antipromastigote activity, 0.4 < SpI < 2.0 indicates activity against both forms, SpI > 2.0 indicates more anti-amastigote activity.[55] [d] Specificity index of *L. major*: SpI_1 = IC_{50} promastigote/IC_{50} amastigote. Selectivity Indexes of *L. donovani*.

Against *L. donovani*, azines **4a**, **6a**, **9a**, **1b** and **8b** displayed with cidal anti-amastigote activity against antimonial-resistant *L. donovani*.[61,62] Of these, **4a**, **6a**, **9a** and **8b** qualified as antileishmanial hits (IC_{50} < 10 μM; SI > 10).[52] However, **8a** and **1b** presented with moderate to significant cytotoxicity against Vero and host THP-1 cells and therefore do not stand as antileishmanial hits. Compound **9a** had submicromolar anti-amastigote activity and a favourable selectivity index, which qualify it as an antileishmanial hit despite its toxicity. Overall, azines, **4a**, **6a**, **8a** and **1b** did not improve on the activity of the reference compounds and AmB. However, they exhibit specificity towards the parasite. Azines **4a** and **6a** presented with affinity for both parasite developmental forms while **8a** and **1b** acted more selectively against the promastigotes. On the other hand, the activity of **9a** and **8b** improved significantly compared to those of the reference drugs with both compounds being selective towards the amastigote form (SpI > 2).[55] Their toxicity, however, was higher than those of the reference drugs. Conversely, azine **7a** qualified as potential antileishmanial lead (IC_{50} < 1 μM; SI > 100)[52] with specificity towards the amastigote form, significantly improving on the cytotoxicity and antileishmanial activity of the reference drugs, including AmB (though marginally) against antimonial-resistant *L. donovani*.

Table 3 Antileishmanial activities and cytotoxicity (μM ± standard deviation) of compounds against *L. donovani* strain 9515

Compd.	Anti-promastigote activity		Anti-amastigote activity			
	IC_{50} (μM)	SI_4[a]	IC_{50} (μM)	SI_5[b]	SI_6[c]	SpI_2[d]
NFA	>10	—	2.68 ± 0.68	2	30	—
1a	1.45 ± 0.19	11	>10	—	—	—
2a	1.18 ± 0.14	40	>10	—	—	—
3a	0.67 ± 0.04	149	>10	—	—	—
4a	3.56 ± 0.00	28	6.41 ± 0.00	16	16	0.56
5a	0.76 ± 0.05	132	>10	—	—	—
6a	1.16 ± 0.11	44	2.28 ± 0.07	22	44	0.51
7a	1.61 ± 0.22	62	0.25 ± 0.09	400	400	6.44
8a	1.02 ± 0.08	18	2.70 ± 0.62	7	17	0.38
9a	0.70 ± 0.06	17	0.53 ± 0.22	22	32	1.32
NTA	5.07 ± 0.45	2	>10	—	—	—
1b	0.93 ± 0.06	45	7.26 ± 2.56	6	14	0.13
2b	2.00 ± 0.15	50	>10	—		—
8b	1.66 ± 0.18	20	0.34 ± 0.03	97	67	4.88
11	>10		>10			
12	>10		>10			
NFZ	1.85 ± 0.14	54	1.69 ± 0.36	59	—	1.09
FZD	0.28 ± 0.28	357	2.70 ± 0.81	37	—	0.10
AmB	0.02 ± 0.009	2890	0.45 ± 0.05	128	—	0.04

[a] SI_4 = IC_{50} Vero/IC_{50} promastigote. [b] SI_5 = IC_{50} Vero/IC_{50} amastigote. [c] SI_6 = IC_{50} THP-1/IC_{50} amastigote. [d] Specificity index of *L. donovani*: SpI_2 = IC_{50} promastigote/IC_{50} amastigote. Selectivity indexes of *T. cruzi*.

To confirm that the nitrofuran moiety serves as pharmacophore, analogues of a small selection of the most active antileishmanial compounds were synthesised and screened for antiparasitic activity and cytotoxicity. Omission of the nitro-substituent in the nitrofuran moiety of the antileishmanial hits **7a** and **9a**, resulted in azines **11** and **12**, respectively, that displayed a complete loss of both anti-

Table 4 Antitrypanosomal activities (μM ± standard deviation) of compounds against *T. cruzi* strain CL

Compd.	Anti-epimastigote activity		Anti-trypomastigote activity			
	IC_{50} (μM)	SI_5[a]	IC_{50} (μM)	SI_6[b]	SI_7[c]	SpI_3[d]
NFA	>10	—	>10	—	—	—
1a	7.66 ± 0.37	2	2.31 ± 0.11	7	42	3.32
2a	3.56 ± 0.46	13	1.95 ± 0.09	24	51	3.32
3a	2.41 ± 0.05	41	3.05 ± 0.06	33	33	0.79
4a	46.15 ± 9.12	2	>10	—	—	—
5a	3.69 ± 0.60	27	4.04 ± 0.09	25	25	0.91
6a	4.92 ± 0.47	10	6.14 ± 0.01	8	16	0.80
7a	95.24 ± 4.03	1	>10	—	—	—
8a	7.30 ± 2.77	3	1.74 ± 0.01	11	27	4.20
9a	2.63 ± 0.01	4	0.78 ± 0.01	15	21	3.37
NTA	>10	—	1.62 ± 0.05	8	16	—
1b	9.21 ± 1.03	5	2.50 ± 0.05	17	40	3.68
2b	>10	—	6.56 ± 0.22	15	15	—
8b	>10	—	3.04 ± 0.06	11	8	—
11	>10	—	>10			
12	>10	—	>10			
NFZ	7.83 ± 1.04	13	2.23 ± 0.06	45	45	3.51
FZD	2.01 ± 0.41	50	3.30 ± 0.25	30	30	0.61
Bzn	—	—	4.79 ± 0.56	21	21	—

[a] SI_5 = IC_{50} Vero/IC_{50} epimastigote. [b] SI_6 = IC_{50} Vero/IC_{50} trypomastigote. [c] SI_7 = IC_{50} THP-1/IC_{50} trypomastigote. Specificity index (SpI) < 0.4 indicates more anti-epimastigote activity, 0.4 < SpI < 2.0 indicates activity against both forms, SpI > 2.0 indicates more antitrypomastigote activity.[55] [d] Specificity index of *T. cruzi*: SpI_3 = IC_{50} epimastigote/IC_{50} trypomastigote. Vero: African green monkey kidney epithelial cells; blue = compounds qualifying as antileishmanial/antitrypanosomal hits;[52] red = compounds qualifying as potential antileishmanial leads.[52] All data reported in the tables were significant at $p < 0.05$. NFA: 5-nitro-2-furaldehyde; NTA: 5-nitro-2-thiophenecarboxaldehyde; FZD: furazolidone; NFZ: nitrofurazone; Em: emetine; Bzn: benznidazole; AmB: amphotericin B; —: not determined; >10: compound did not qualify for IC_{50} determination due to low growth inhibition presented during single-point screening.

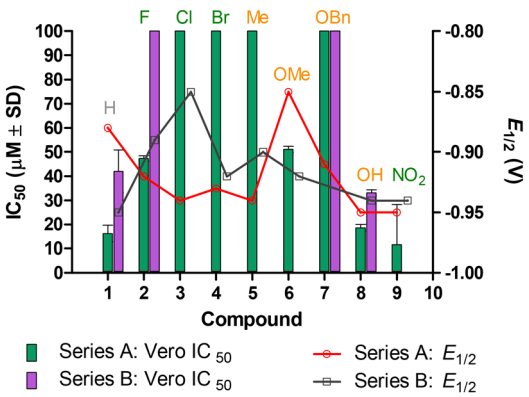

Fig. 5 Comparison of general cytotoxicity in Vero and electrochemistry. EWGs are indicated in green, whereas EDGs were indicated in orange and the neutral group was indicated in grey.

amastigote activity (IC_{50} > 10 μM) and the cytotoxicity (IC_{50} > 100 μM) (Tables 2 and 3). The latter confirmed the nitro group acting as toxicophore.

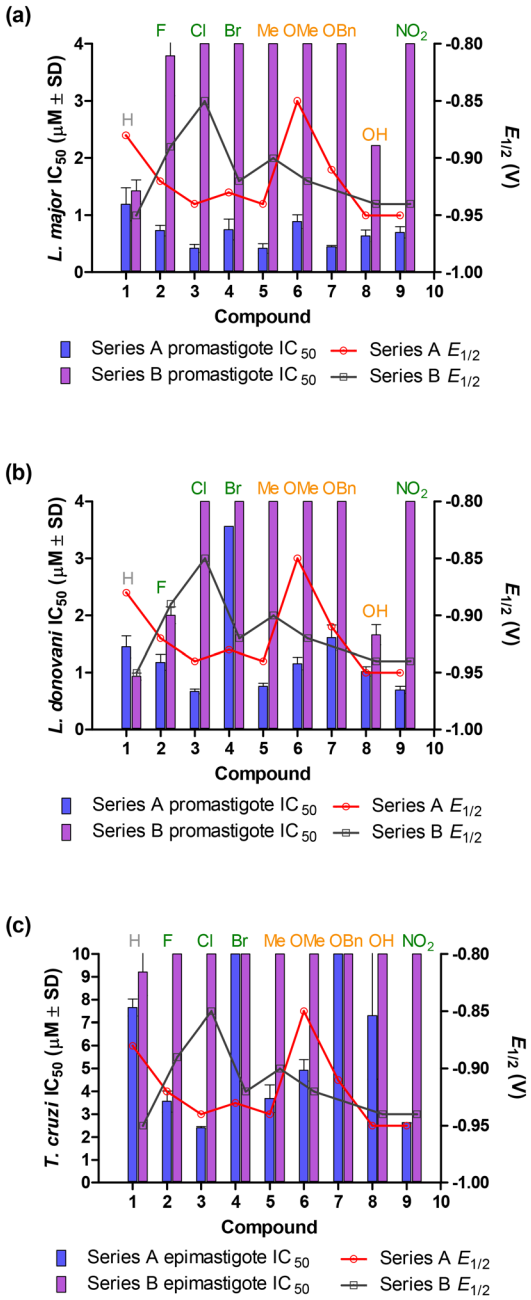

Fig. 6 Comparison of antipromastigote and anti-epimastigote activities and electrochemistry. (a) Antipromastigote activity of *L. major* strain IR-173. (b) Antipromastigote activity of *L. donovani* strain 9515. (c) Anti-epimastigote activity of *T. cruzi* strain CL. EWGs are indicated in green, whereas EDGs were indicated in orange and the neutral group was indicated in grey.

Antitrypanosomal activity. Several azines, including **1a–3a**, **5a**, **6a**, **8a**, **9a**, **1b**, **2b** and **8b**, presented with activity against *T. cruzi* trypomastigotes, the human infective and non-proliferating form of the parasite. As already stated, there are no specific guidelines to identify hit/lead compounds for the trypomastigote form. Thus, the guidelines for *T. cruzi* anti-amastigote activity of Katsuno *et al.*,[52] which are identical to those of *Leishmania* anti-amastigote activity, were applied. All

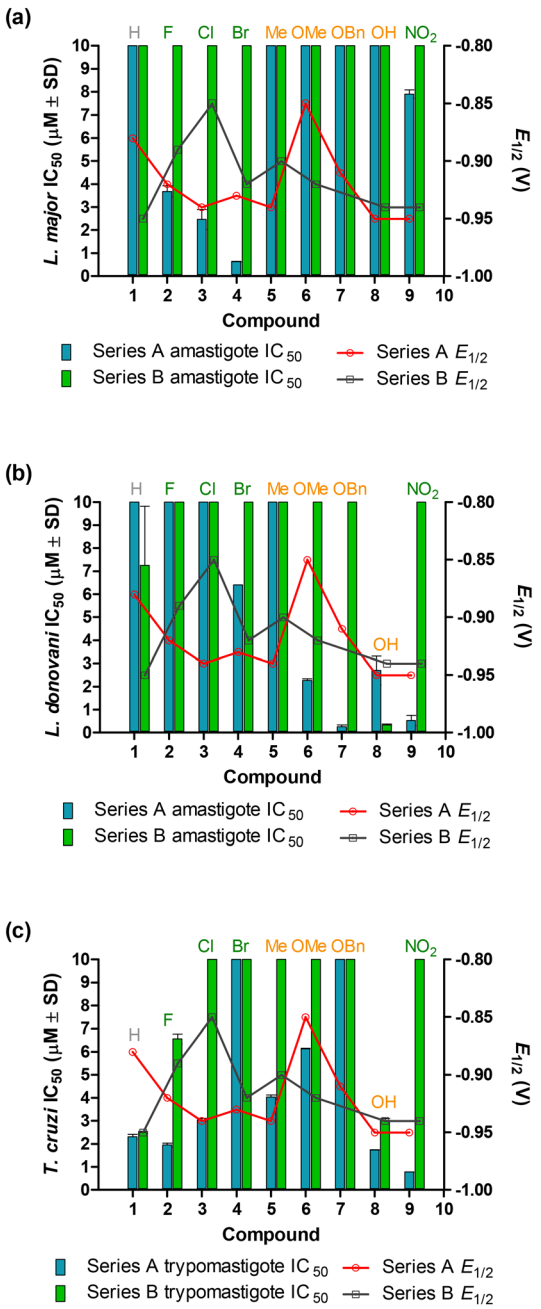

Fig. 7 Comparison of anti-amastigote and antitrypomastigote activities and electrochemistry. (a) Anti-amastigote activity of *L. major* strain IR-173. (b) Anti-amastigote activity of *L. donovani* strain 9515. (c) Antitrypomastigote activity of *T. cruzi* strain CL. EWGs are indicated in green, whereas EDGs were indicated in orange and the neutral group was indicated in grey.

the active compounds, apart from **1a** and **6a**, qualified as antitrypanosomal hits (IC_{50} < 10 μM; SI > 10).[52] When applying De Muylder *et al.*'s[55] specificity index using the anti-epimastigote and antitrypomastigote data, azines **1a**, **2a**, **8a**, **9a**, **1b**, **2b** and **8b** had their activity directed selectively towards the trypomastigote form (SpI > 2), whereas **3a**, **5a** and **6a** were active against both epimastigote and trypomastigote forms (0.4 < SpI < 2.0) (Fig. 7). Overall, nitrofuran aldazine **9a** (IC_{50} < 1 μM; SI < 100) with submicromolar antitrypomastigote activity was identified as hit and the most promising antitrypanosomal of the study, falling short of being an early lead due to lower selectivity for the trypomastigote of *T. cruzi*.

Similarly, to the loss of antileishmanial activity, the analogue **12** of the antitrypanosomal cytotoxic hit **9a**, also resulted in a complete loss of both anti-trypomastigote activity and cytotoxicity (Table 3), confirming the nitrofuran moiety as both pharmacophore and toxicophore for this nitrofuranylazine.

Structure–activity relationships (SARs). Furan and thiophene are heterocyclic synthons that differ by their chalcogen atoms, oxygen, and sulphur, respectively. In the present study, the antiprotozoal activities of both subseries of azines were compared. The nitrofuran sub-series (**1a–9a**) exhibited much more potent activity than its nitrothiophene counterparts (**1b–9b**). This may be explained by the presence of nitrofuran's hydrogen bond acceptor *i.e.*, O atom. Indeed, hydrogen bonds are significant in both medicinal and biochemistry. These bonds are important because a single hydrogen bond interaction can enhance the potency of oxygen-containing drugs towards parasites in comparison to their sulphur containing counterparts.[63]

Due to the limited biological activity of the nitrothiophene azines, no correlations were detected between antiparasitic activity and electrochemical data. However, except for azines **7a**, **8a** and **9a**, there was a visible correlation between the antiparasitic (*Leishmania* antipromastigote and *T. cruzi* anti-epimastigote) IC_{50} of the nitrofuranylazines and their $E_{1/2}$ values (Fig. 6). This was in line with the following electronic effect observations, confirming a correlation between the electrochemical characteristics of the compounds and the resulting antipromastigote and anti-epimastigote activities.

Furthermore, due to a lack of significant differences between the IC_{50} ranges of the EDG and EWG-containing compounds, it was not possible to sufficiently determine whether the compounds' tendency to be reduced affected their resulting antipromastigote and anti-epimastigote activities.

When considering the electronic effect and strength, the R groups on the Ph ring can be divided, and in order of increasing strength, into EWGs (Br < Cl < F < NO_2), neutral groups (H), and EDGs (CH_3(Me) < OH < OCH_3(OMe) < $OCH_2C_6H_5$(OBn).

The general pattern observed for EWG-containing azines against *L. major* IR-173 (Fig. 6a) consists of an increase in antipromastigote activity (though marginally) as the strength of the EWG increases (except **3a**). This is evident by the activity of **9a**, bearing the strongest of these EWGs (*i.e.*, NO_2), that exhibits IC_{50} 0.70 μM, compared to 0.75 μM of **4a** that has the weakest EWG (*i.e.*, Br). The EDG-harbouring azines, on the other hand, display a marginal decrease in activity as the strength of the EDG increases (Fig. 6a). This can be seen by the strongest of these EDGs (the OBn group), azine **7a**, exhibiting an IC_{50} 0.45 μM, compared to 0.42 μM of the

weakest EDG Me-bearing azine **5a**. The neutral group, H-containing **1a** exhibited the weakest antipromastigote activity, with an IC_{50} value of 1.19 μM.

Scrutiny of the activity against *L. donovani* 9515 promastigotes shows a broadly evident trend similar to that of *L. major* (Fig. 4b), with an increase in activity of EWG azines as the electronic effect strengthens. The increasing activity order was: **4a** (IC_{50} 3.56 μM) < **2a** (IC_{50} 1.18 μM) < **9a** (IC_{50} 0.70 μM) with **3a** (IC_{50} 0.67 μM) being an outlier. The same trend is evident with the EDG azines, where a decrease in activity is observed with an increase in electronic strength in the order: **5a** (IC_{50} 0.76 μM), **8a** (IC_{50} 1.02 μM), **6a** (IC_{50} 1.16 μM) and **7a** (IC_{50} 1.61 μM). Thus, the strongest EDG containing azine **7a** had the weakest activity while the weakest EDG bearing **5a** possessed the strongest antipromastigote activity. The neutral group bearing **1a** exhibited the second weakest activity (IC_{50} 1.45 μM) of the subseries against *L. donovani*.

Analysis of the activity against *T. cruzi* reveals that the neutral **1a** again exhibits weaker activity (IC_{50} 7.66 μM). With the EWG azines, an increase in activity followed an increase in electronic strength, **3a** being an outlier, as seen with the antipromastigote activities (Fig. 6c). The EDG-harbouring nitrofuranylazines also displayed the same trend of activity against *T. cruzi* as with *L. major*, where a decrease in activity is observed with an increase in electronic strength, azine **8a** being the exception (Fig. 6c). Fig. 8 depicts the summary of SAR in this study.

With regards to the more clinically relevant parasite forms, there were no visible correlations between the antiparasitic IC_{50} values and $E_{1/2}$ values (Fig. 7). However, there were several seemingly species and/or parasite form-dependent correlations between the antiparasitic activities and compound electronic effects.

In *Leishmania* amastigotes, azines **1** (*i.e.*, **1a** & **1b**) with neutral group generally presented with IC_{50} > 7 μM. For *L. major*, an increase in EWG strength in nitrofuran derivatives resulted in significantly decrease anti-amastigote activity compared to **1a** and non-significant nitrothiophene derivative activity when compared to **1b** (Fig. 7a), whereas in *L. donovani* this activity and pattern were lost in both series (Fig. 7b). The addition of EDGs, on the other hand, did not improve activity against *L. major*, whereas an increase in nitrofuran derivative EDG strength resulted in an increase in activity against *L. donovani* amastigotes. These observations contrast with the observations of the antipromastigote activities.

In *T. cruzi* trypomastigotes, azines **1** (**1a** & **1b**) were significantly more active (IC50 < 2.5 μM) than in *Leishmania*. An increase in EWG strength resulted in increased nitrofuran derivative anti-trypomastigote activity, whereas an increase in EDG strength resulted in activity, with the exception of **5a**, but no clear patterns for the nitrothiophene series (Fig. 7c). These observations are in line with the observations of the anti-epimastigote activities.

Fig. 8 depicts a summary of discovered SAR of the study.

Bioisosterism. Bioisosterism plays a very important role in medicinal chemistry. Bioisosteres are defined as molecules or groups with similar physical and chemical properties that exhibit similar biological characteristics.[64] Some of the main benefits of bioisosterism include the logical modification of lead molecules into compounds that are safer and more effective by reducing toxicity, modifying activity, and adapting pharmacokinetics.[65] In this study, several classical bioisosteres were applied, such as ring equivalents (nitrofuran and nitrothiophene), as well as monovalent bioisosteres (*e.g.*, Cl and Br).

When comparing ring equivalents **1a** and **1b**, there was comparable lipophilicity with log $P_{o/w}$ values of 2.01 and 2.66, respectively. However, differences in toxicity and activity against all parasite strains were observed, with **1a** being more potent against *L. major* and *T. cruzi*, while **1b** was more potent against *L. donovani*.

Comparison of bioisosteres **3a** and **4a**, revealed that both azines had comparable lipophilicity with log $P_{o/w}$ values of 2.52 and 2.64, respectively, and were found to be non-toxic to mammalian cells, but exhibited different activity against parasites, with **3a** being the more potent azine. Therefore, bioisosterism proved beneficial in this study.

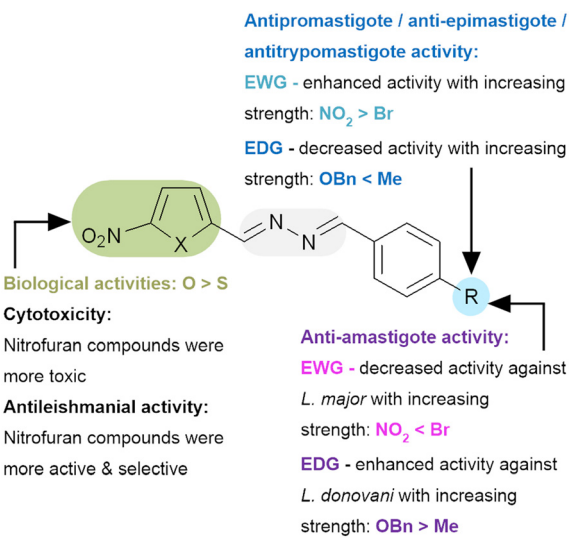

Fig. 8 Summary of uncovered SAR of the study.

Conclusions

Post COVID-19, there has been significant interest in the development of multifunctional, broad-spectrum antipathogenic drugs to improve global responsiveness to non-traditional diseases and future health emergencies.[66] Furthermore, broad-spectrum antipathogenic drugs can also address the logistical and economic challenges associated with infectious diseases with overlapping geographical distributions.[67] Accordingly, this study utilised the multifunctional clinical nitrofuran scaffold as pharmacophore to synthesise new nitrofuran derivatives with

the aim of improving its biological antiparasitic activity. A series of nitrofuran-based azines were synthesised in poor to excellent yields following a two-step process that included hydrazone formation and a Schiff base reaction. Most of the compounds were found to have low cytotoxicity, apart from a handful that exhibited moderate toxicity. It was observed that the nitrofuran sub-series was more potent than the nitrothiophene sub-series, having due favourable electrochemical properties like nifurtimox. Additionally, the superior activity of nitrofuranylazines might be related to the oxygen atom of the furan ring's ability to form hydrogen bonds. The electronic effect analysis showed species and parasite form-specific effects. Nitrofuranylazines, **4a** and **7a** were uncovered as safe antileishmanial early leads while **9a** stood out as a trypanocidal hit. All three azines will undergo future investigation to dissect their exact mechanism of action and to identify their molecular targets within the parasites. It will also be worth establishing whether the promising *in vitro* parasiticidal activity can be translated *in vivo*. Furthermore, nitrofuran was confirmed as the pharmacophore as analogues (**11**, **12**) of the most active derivatives (**7a**, **9a**), wherein the nitro-group of the nitrofuran was removed, presented with a complete loss in biological activity. Moreover, the antiparasitic activities of the synthesised azines were compared and hits, **2a**, **3a**, **9a** and **8b** were identified as potential dual-active compounds due to their activity against both *Leishmania* and *T. cruzi*. These parasite species are, however, taxonomically related, and accordingly share similar biochemical and structural characteristics. Further assessment against non-related pathogens will therefore be required to determine their broad-spectrum antiparasitic activity. In theory, there is potential for broad-spectrum activity as the nitrofuran pharmacophore is known to promote oxidative stress, a species-independent drug target.

Further, this study focused exclusively on unsymmetrical aromatic azines that proved to be cytotoxic in general due to their lipophilicity. Hence, it will be of interest in future endeavour to explore nitrofuran azines containing less lipophilic building blocks, alkyl, heterocycles *etc.*

Experimental section

Materials

All reagents used were purchased from Sigma-Aldrich (Johannesburg, South Africa), and solvents from Associated Chemical Enterprises, ACE (South Africa). All chemicals and reagents were of analytical grade, and as such, no further purification was needed.

General procedures

The ^{1}H and ^{13}C nuclear magnetic resonance (NMR) spectra were recorded on a Bruker Avance™ III 600 spectrometer at a frequency of 600 and 151 MHz, respectively, in deuterated dimethyl sulfoxide (DMSO-d_6). The chemical shifts were reported in parts per million (ppm) with the residual protons of the solvent as a reference. The abbreviations of the splitting patterns were as follows: singlet (s), doublet (d), doublet of doublet (dd), doublet of triplets (dt), triplet (t), triplet of doublets (td), triplet of triplets (tt), quartet of doublets (qd), and multiplet (m). High resolution mass spectrometry (HRMS) spectra were recorded on a Bruker MicroTOF Q II mass spectrometer. It was equipped with an atmospheric pressure chemical ionisation (APCI) source set at 200 °C or 180 °C and analysed using Bruker Compass Data Analysis 4.0 software. A full scan ranged from 50–1500 m/z at a capillary voltage of 4500 V, an end plate offset voltage of −500 V, with the nebuliser set at 1.6 and 0.4 bar, respectively, and a collision cell RF voltage of 100 Vpp. Infrared (FTIR) spectra were recorded on a Bruker Alpha-P FTIR instrument. A BÜCHI melting point B-545 instrument was used to determine melting points (mp) and were uncorrected. Thin layer chromatography (TLC) was performed on silica gel plates ($60F_{254}$) that were acquired from Merck (South Africa).

Syntheses

Phenylhydrazones (1–8). Substituted phenylaldehyde (10 mmol, 1 eq.) was dissolved in dichloromethane (DCM, 10 mL); triethylamine (TEA, 15 mmol, 1.5 eq., 1.4 mL) was added, and the reaction was left to stir at room temperature for 10 minutes. Thereafter, excess hydrazine monohydrate (60 mmol, 6 eq., 2.9 mL) was added, and the reaction mixture was stirred at room temperature for another 12 hours upon monitoring by TLC eluting with hexane : ethyl acetate (EtOAc) (7 : 3, v/v or 1 : 1 v/v). Upon completion, the reaction mixture was extracted with DCM (2 × 30 mL) and water (2 × 40 mL). The organic phase was dried over anhydrous magnesium sulphate ($MgSO_4$), filtered, and concentrated *in vacuo* to yield a crude product, which was then recrystallised in EtOAc to form the phenylhydrazone. Characterisation data for all the intermediates is reported as ESI.†

Phenylhydrazone (9). 4-Nitrobenzaldehyde (10 mmol, 1 eq.) was dissolved in ethanol (20 mL) and then hydrazine monohydrate (70 mmol, 7 eq., 3.4 mL) and *p*-toluenesulfonic acid (PTSA, 1 mmol, 0.08 eq.) were added consecutively. The reaction was refluxed for 60 minutes and monitored by TLC. Upon completion, it was cooled down to 5–10 °C and the precipitate formed was filtered, washed with cold water and dried under vacuum to yield intermediate **9** used in subsequent reactions without further purification.

Azine derivatives (1a–9a & 1b–9b). 5-Nitro-2-furaldehyde or 5-nitro-2-thiophenecarboxaldehyde (3 mmol, 1 eq.) was dissolved in anhydrous ethanol (10 mL) upon stirring and then substituted phenylhydrazone (3 mmol, 1 eq.) and 1 drop of catalytic sulphuric acid were added. The reaction mixture was stirred for 12 hours and monitored by TLC eluting with Hex : EtOAc (7 : 3, v/v or 1 : 1 v/v). Upon completion, the reaction was quenched with water (50 mL) and the precipitate that formed was filtered and recrystallised from EtOAc to afford the desired azines (**1a–9a**, **1b–9b**). Compounds **6a** and **7b** were further purified by column

chromatography on silica gel eluting with Hex : EtOAc (4 : 1, v/v).

In the case of azines, **5a**, **9a**, **5b**, **6b** and **9b**, the acid method was found unsuitable as the product could not be formed, hence the sulphuric acid was substituted for anhydrous potassium carbonate (6 mmol, 2 eq.).

Characterisation spectra of all compounds are provided as ESI.†

(1E,2E)-1-Benzylidene-2-[(5-nitrofuran-2-yl)methylene] hydrazine ***1a***. Brown powder. Yield: 715 mg (98%); mp 169–171 °C; R_f 0.7 (Hex : EtOAc 1 : 1, v/v). IR ν_{max} (cm^{-1}): 1629 (C═N), 1565 (C═C), 1471 (N–O), 1246 (C–O); ^{1}H NMR (DMSO-d_6, 600 MHz) δ (ppm): 8.78 (s, 1H, H-1′), 8.64 (s, 1H, H-6), 7.90 (d, J = 6.9 Hz, 2H, H-3′), 7.81 (d, J = 3.8 Hz, 1H, H-4), 7.56 (t, J = 7.1 Hz, 1H, H-5′), 7.53 (d, J = 6.9 Hz, 2H, H-4′), 7.40 (d, J = 3.8 Hz, 1H, H-3); ^{13}C NMR (DMSO-d_6, 151 MHz) δ (ppm): 163.8, 152.5, 150.7, 149.6, 133.3, 132.0, 129.0, 128.8, 118.5, 114.1. HRMS-APCI (*pos*) m/z 244.0717 $[M + H]^+$ (Calcd. for $C_{12}H_9N_3O_3^+$, 244.0722).

(1E,2E)-1-(4-Fluorobenzylidene)-2-[(5-nitrofuran-2-yl) methylene]hydrazine ***2a***. Yellow powder. Yield: 517 mg (66%); mp 191–193 °C; R_f 0.39 (Hex : EtOAc 7 : 3, v/v). IR ν_{max} (cm^1): 3113 (C–H), 1631 (C═N), 1597 (C═C), 1516 (N–O), 1342 (C–F), 1247 (C–O); ^{1}H NMR (DMSO-d_6, 600 MHz) δ (ppm): 8.81 (s, 1H, H-1′), 8.65 (s, 1H, H-6), 7.97 (dd, J_{H-F} = 8.8, 5.7 Hz, 2H, H-3′), 7.82 (d, J = 3.9 Hz, 1H, H-4), 7.41 (d, J = 3.9 Hz, 1H, H-3), 7.38 (t, J_{H-F} = 8.8 Hz, 2H, H-4′); ^{13}C NMR (DMSO-d_6, 151 MHz) δ (ppm): 164.2 (d, $^1J_{C-F}$ = 250.3 Hz), 162.6, 151.4, 150.6, 149.6, 131.2 (d, $^2J_{C-F}$ = 9.1 Hz), 130.0 (d, $^3J_{C-F}$ = 2.9 Hz), 118.5, 116.2 (d, $^4J_{C-F}$ = 22.0 Hz), 114.1. HRMS-APCI (*pos*) m/z 262.0635 $[M + H]^+$ (Calcd. for $C_{12}H_8FN_3O_3^+$, 262.0628).

(1E,2E)-1-(4-Chlorobenzylidene)-2-[(5-nitrofuran-2-yl) methylene]hydrazine ***3a***. Yellow powder. Yield: 500 mg (60%); mp 175–177 °C; R_f 0.53 (Hex : EtOAc 7 : 3, v/v). IR ν_{max} (cm^{-1}): 3092 (C–H), 1630 (C═N), 1562 (C═C), 1352 (N–O), 1246 (C–O), 820 (C–Cl); ^{1}H NMR (DMSO-d_6, 600 MHz) δ (ppm): 8.81 (s, 1H, H-1′), 8.65 (s, 1H, H-6), 7.92 (d, J = 8.5 Hz, 2H, H-3′), 7.82 (d, J = 3.9 Hz, 1H, H-4), 7.61 (d, J = 8.5 Hz, 2H, H-4′), 7.42 (d, J = 3.9 Hz, 1H, H-3); ^{13}C NMR (DMSO-d_6, 151 MHz) δ (ppm): 162.6, 152.5, 150.6, 149.8, 136.6, 132.2, 130.3, 129.2, 118.7, 114.1. HRMS-APCI (*pos*) m/z 278.0334 $[M + H]^+$ (Calcd. for $C_{12}H_8ClN_3O_3^+$, 278.0332).

(1E,2E)-1-(4-Bromobenzylidene)-2-[(5-nitrofuran-2-yl) methylene]hydrazine ***4a***. Yellow powder. Yield: 754 mg (78%); mp 196–198 °C; R_f 0.55 (Hex : EtOAc 7 : 3, v/v). IR ν_{max} (cm^{-1}): 3092 (C–H), 1629 (C═N), 1563 (C═C), 1475 (N–O), 1243 (C–O), 513 (C–Br); ^{1}H NMR (DMSO-d_6, 600 MHz) δ (ppm): 8.79 (s, 1H, H-1′), 8.65 (s, 1H, H-6), 7.84 (d, J = 8.5 Hz, 2H, H-3′), 7.82 (d, J = 3.9 Hz, 1H, H-4), 7.75 (d, J = 8.5 Hz, 2H, H-4′), 7.42 (d, J = 3.9 Hz, 1H, H-3); ^{13}C NMR (DMSO-d_6, 151 MHz) δ (ppm): 162.7, 152.6, 150.6, 149.8, 132.5, 132.1, 130.5, 125.6, 118.7, 114.1. HRMS-APCI (*pos*) m/z 321.9824 $[M + H]^+$ (Calcd. for $C_{12}H_8BrN_3O_3^+$, 321.9827).

(1E,2E)-1-(4-Methylbenzylidene)-2-[(5-nitrofuran-2-yl) methylene]hydrazine ***5a***. Yellow powder. Yield: 100 mg (13%); mp 167–169 °C; R_f 0.68 (Hex : EtOAc 7 : 3, v/v). IR ν_{max} (cm^{-1}): 3118 (C–H), 1626 (C═N), 1571 (C═C), 1336 (N–O), 1241 (C–O); ^{1}H NMR (DMSO-d_6, 600 MHz) δ (ppm): 8.76 (s, 1H, H-1′), 8.64 (s, 1H, H-6), 7.82 (d, J = 3.9 Hz, 1H, H-4), 7.79 (d, J = 8.1 Hz, 2H, H-3′), 7.39 (d, J = 3.9 Hz, 1H, H-3), 7.34 (d, J = 8.1 Hz, 2H, H-4′), 2.38 (s, 3H, H-6′); ^{13}C NMR (DMSO-d_6, 151 MHz) δ (ppm): 163.9, 152.5, 150.8, 149.3, 142.3, 130.6, 129.6, 128.8, 118.3, 114.1, 21.2. HRMS-APCI (*pos*) m/z 258.0880 $[M + H]^+$ (Calcd. for $C_{13}H_{11}N_3O_3^+$, 258.0879).

(1E,2E)-1-(4-Methoxybenzylidene)-2-[(5-nitrofuran-2-yl) methylene]hydrazine ***6a***. Orange powder. Yield: 221 mg (27%); mp 169–171 °C; R_f 0.35 (Hex : EtOAc 7 : 3, v/v). IR ν_{max} (cm^{-1}): 2921 (C–H), 1706 (C═N), 1600 (C═C), 1347 (N–O), 1239 (C–O); ^{1}H NMR (DMSO-d_6, 600 MHz) δ (ppm): 8.75 (s, 1H, H-1′), 8.62 (s, 1H, H-6), 7.86 (d, J = 8.8 Hz, 2H, H-3′), 7.82 (d, J = 3.9 Hz, 1H, H-4), 7.38 (d, J = 3.9 Hz, 1H, H-3), 7.09 (d, J = 8.8 Hz, 2H, H-4′), 3.84 (s, 3H, H-6′); ^{13}C NMR (DMSO-d_6, 151 MHz) δ (ppm): 163.8, 162.4, 151.0, 148.9, 130.7, 125.9, 118.0, 114.6, 114.6, 114.2, 55.5. HRMS-APCI (*pos*) m/z 274.0840 $[M + H]^+$ (Calcd. for $C_{13}H_{11}N_3O_4^+$, 274.0828).

(1E,2E)-1-[4-(Benzyloxy)benzylidene]-2-[(5-nitrofuran-2-yl) methylene]hydrazine ***7a***. Yellow powder. Yield: 786 mg (75%); mp 175–177 °C; R_f 0.59 (Hex : EtOAc 7 : 3, v/v). IR ν_{max} (cm^{-1}): 3102 (C–H), 1618 (C═N), 1573 (C═C), 1352 (N–O), 1246 (C–O); ^{1}H NMR (DMSO-d_6, 600 MHz) δ (ppm): 8.74 (s, 1H, H-1′), 8.61 (s, 1H, H-6), 7.86 (d, J = 8.8 Hz, 2H, H-3′), 7.80 (d, J = 3.9 Hz, 1H, H-4), 7.47 (d, J = 7.5 Hz, 2H, H-8′), 7.41 (t, J = 7.5 Hz, 2H, H-9′), 7.37 (d, J = 3.9 Hz, 1H, H-3), 7.35 (t, J = 7.5 Hz, 1H, H-10′), 7.16 (d, J = 8.8 Hz, 2H, H-4′), 5.21 (s, 2H, H-6′); ^{13}C NMR (DMSO-d_6, 151 MHz) δ (ppm): 163.5, 161.4, 152.3, 150.9, 148.7, 136.5, 130.6, 128.4, 127.9, 127.7, 126.0, 117.9, 115.3, 114.1, 69.5. HRMS-APCI (*pos*) m/z 350.1151 $[M + H]^+$ (Calcd. for $C_{19}H_{15}N_3O_4^+$, 350.1141).

4-{(E)-{(E)-[(5-Nitrofuran-2-yl)methylene]hydrazono}methyl} phenol ***8a***. Red powder. Yield: 109 mg (14%); mp 216–218 °C; R_f 0.39 (Hex : EtOAc 1 : 1, v/v). IR ν_{max} (cm^{-1}): 3426 (O–H), 3112 (C–H), 1598 (C═N), 1565 (C═C), 1347 (N–O), 1211 (C–O); ^{1}H NMR (DMSO-d_6, 600 MHz) δ (ppm): 10.27 (s, 1H, H-6′), 8.69 (s, 1H, H-1′), 8.59 (s, 1H, H-6), 7.81 (d, J = 3.9 Hz, 1H, H-4), 7.75 (d, J = 8.6 Hz, 2H, H-3′), 7.35 (d, J = 3.9 Hz, 1H, H-3), 6.89 (d, J = 8.6 Hz, 2H, H-4′); ^{13}C NMR (DMSO-d_6, 151 MHz) δ (ppm): 164.2, 161.3, 152.4, 151.1, 148.4, 131.0, 124.3, 117.8, 115.9, 114.2. HRMS-APCI (*pos*) m/z 260.0686 $[M + H]^+$ (Calcd. for $C_{12}H_9N_3O_4^+$, 260.0671).

(1E,2E)-1-(4-Nitrobenzylidene)-2-[(5-nitrofuran-2-yl)methylene] hydrazine ***9a***. Light brown powder. Yield: 536 mg (62%); mp 170–172 °C; R_f 0.42 (Hex : EtOAc 7 : 3, v/v). IR ν_{max} (cm^{-1}): 3111 (C–H), 1633 (C═N), 1572 (C═C), 1526 (N–O), 1342 (N–O), 1251 (C–O); ^{1}H NMR (DMSO-d_6, 600 MHz) δ (ppm): 8.92 (s, 1H, H-1′), 8.69 (s, 1H, H-6), 8.37 (d, J = 8.7 Hz, 2H, H-4′), 8.15 (d, J = 8.7 Hz, 2H, H-3′), 7.83 (*d, J = 3.9 Hz, 1H, H-4), 7.46 (*d, J = 3.9 Hz, 1H, H-3); ^{13}C NMR (DMSO-d_6, 151 MHz) δ (ppm): 161.4, 150.5, 150.3, 149.1, 139.2, 137.5, 129.7, 124.1, 119.3, 114.0. HRMS-APCI (*pos*) m/z 289.0577 $[M + H]^+$ (Calcd. for $C_{12}H_8N_4O_5^+$, 289.0573). *d is a coalesced doublet.

(1E,2E)-1-Benzylidene-2-[(5-nitrothiophen-2-yl)methylene] hydrazine ***1b***. Yellow powder. Yield: 436 mg (56%); mp 166–

168 °C; R_f 0.63 (Hex : EtOAc 7 : 3, v/v). IR ν_{max} (cm^{-1}): 3096 (C–H), 1610 (C=N), 1531 (C=C), 1495 (N–O); ^{1}H NMR (DMSO-d_6, 600 MHz) δ (ppm): 8.94 (s, 1H, H-1′), 8.75 (s, 1H, H-6), 8.19 (d, J = 4.3 Hz, 1H, H-4), 7.90 (d, J = 7.5 Hz, 2H, H-3′), 7.72 (d, J = 4.3 Hz, 1H, H-3), 7.56 (d, J = 7.5 Hz, 1H, H-5′), 7.52 (d, J = 7.5 Hz, 2H, H-4′); ^{13}C NMR (DMSO-d_6, 151 MHz) δ (ppm): 163.6, 155.3, 152.3, 145.0, 133.3, 132.4, 132.0, 130.4, 129.0, 128.8. HRMS-APCI (*pos*) m/z 260.0512 $[M + H]^+$ (Calcd. for $C_{12}H_9N_3O_2S^+$, 260.0494).

(1E,2E)-1-(4-Fluorobenzylidene)-2-[(5-nitrothiophen-2-yl) methylene]hydrazine ***2b***. Yellow powder. Yield: 458 mg (55%); mp 187–189 °C; R_f 0.53 (Hex : EtOAc 7 : 3, v/v). IR ν_{max} (cm^{-1}): 3082 (C–H), 1613 (C=N), 1505 (C=C), 1335 (N–O), 1221 (C–F); ^{1}H NMR (DMSO-d_6, 600 MHz) δ (ppm): 8.93 (s, 1H, H-1′), 8.76 (s, 1H, H-6), 8.19 (d, J = 4.3 Hz, 1H, H-4), 7.97 (dd, J_{H-F} = 8.8, 5.7 Hz, 2H, H-3′), 7.72 (d, J = 4.3 Hz, 1H, H-3), 7.37 (t, J_{H-F} = 8.8 Hz, 2H, H-4′); ^{13}C NMR (DMSO-d_6, 151 MHz) δ (ppm): 164.2 (d, $^1J_{C-F}$ = 250.4 Hz), 162.5, 157.3, 155.4, 152.3, 144.9, 132.4, 131.2 (d, $^2J_{C-F}$ = 9.0 Hz), 130.4, 116.2 (d, $^3J_{C-F}$ = 22.0 Hz). HRMS-APCI (*pos*) m/z 278.0404 $[M + H]^+$ (Calcd. for $C_{12}H_8FN_3O_2S^+$, 278.0400).

(1E,2E)-1-(4-Chlorobenzylidene)-2-[(5-nitrothiophen-2-yl) methylene]hydrazine ***3b***. Yellow powder. Yield: 238 mg (27%); mp 179–181 °C; R_f 0.62 (Hex : EtOAc 1 : 1, v/v). IR ν_{max} (cm^{-1}): 3094 (C–H), 1604 (C=N), 1522 (C=C), 1321 (N–O), 815 (C–Cl); ^{1}H NMR (DMSO-d_6, 600 MHz) δ (ppm): 8.77 (s, 1H, H-1′), 8.57 (s, 1H, H-6), 8.17 (d, J = 4.4 Hz, 1H, H-4), 8.02 (d, J = 8.5 Hz, 2H, H-3′), 7.74 (d, J = 4.4 Hz, 1H, H-3), 7.70 (d, J = 8.5 Hz, 2H, H-4′); ^{13}C NMR (DMSO-d_6, 151 MHz) δ (ppm): 161.8, 156.0, 150.9, 137.1, 136.4, 133.7, 132.0, 130.9, 129.5, 129.1. HRMS-APCI (*pos*) m/z 294.0097 $[M + H]^+$ (Calcd. for $C_{12}H_8ClN_3O_2S^+$, 294.0104).

(1E,2E)-1-(4-Bromobenzylidene)-2-[(5-nitrothiophen-2-yl) methylene]hydrazine ***4b***. Yellow powder. Yield: 416 mg (41%); mp 193–195 °C; R_f 0.21 (Hex : EtOAc 7 : 3, v/v). IR ν_{max} (cm^{-1}): 3083 (C–H), 1610 (C=N), 1550 (C=C), 1332 (N–O), 536 (C–Br); ^{1}H NMR (DMSO-d_6, 600 MHz) δ (ppm): 8.77 (s, 1H, H-1′), 8.59 (s, 1H, H-6), 8.18 (d, J = 4.4 Hz, 1H, H-4), 7.95 (d, J = 8.4 Hz, 2H, H-3′), 7.85 (d, J = 8.4 Hz, 2H, H-4′), 7.75 (d, J = 4.4 Hz, 1H, H-3); ^{13}C NMR (DMSO-d_6, 151 MHz) δ (ppm): 161.9, 156.0, 150.8, 136.3, 133.7, 132.4, 132.3, 131.0, 129.1, 126.2. HRMS-APCI (*pos*) m/z 337.9592 $[M + H]^+$ (Calcd. for $C_{12}H_8BrN_3O_2S^+$, 337.9599).

(1E,2E)-1-(4-Methylbenzylidene)-2-[(5-nitrothiophen-2-yl) methylene]hydrazine ***5b***. Yellow powder. Yield: 197 mg (24%); mp 166–168 °C; R_f 0.66 (Hex : EtOAc 7 : 3, v/v). IR ν_{max} (cm^{-1}): 2920 (C–H), 1609 (C=N), 1532 (C=C), 1327 (N–O); ^{1}H NMR (DMSO-d_6, 600 MHz) δ (ppm): 8.92 (s, 1H, H-1′), 8.71 (s, 1H, H-6), 8.18 (d, J = 4.1 Hz, 1H, H-4), 7.80 (d, J = 8.0 Hz, 2H, H-3′), 7.70 (d, J = 4.1 Hz, 1H, H-3), 7.34 (d, J = 8.0 Hz, 2H, H-4′), 2.38 (s, 3H, H-6′); ^{13}C NMR (DMSO-d_6, 151 MHz) δ (ppm): 163.7, 155.0, 152.2, 145.1, 142.3, 132.2, 130.6, 130.4, 129.6, 128.8, 21.2. HRMS-APCI (*pos*) m/z 274.0644 $[M + H]^+$ (Calcd. for $C_{13}H_{11}N_3O_2S^+$, 274.0650).

(1E,2E)-1-(4-Methoxybenzylidene)-2-[(5-nitrothiophen-2-yl) methylene]hydrazine ***6b***. Orange powder. Yield: 399 mg (46%); mp 171–173 °C; R_f 0.44 (Hex : EtOAc 7 : 3, v/v). IR ν_{max} (cm^{-1}): 2924 (C–H), 1608 (C=N), 1529 (C=C), 1329 (N–O); ^{1}H NMR (DMSO-d_6, 600 MHz) δ (ppm): 8.90 (s, 1H, H-1′), 8.69 (s, 1H, H-6), 8.17 (d, J = 4.3 Hz, 1H, H-4), 7.86 (d, J = 8.7 Hz, 2H, H-3′), 7.68 (d, J = 4.3 Hz, 1H, H-3), 7.08 (d, J = 8.7 Hz, 2H, H-4′), 3.84 (s, 3H, H-6′); ^{13}C NMR (DMSO-d_6, 151 MHz) δ (ppm): 163.5, 162.4, 154.5, 152.0, 145.4, 132.0, 130.7, 130.4, 125.9, 114.6, 55.5. HRMS-APCI (*pos*) m/z 290.0595 $[M + H]^+$ (Calcd. for $C_{13}H_{11}N_3O_3S^+$, 290.0599).

(1E,2E)-1-[4-(Benzyloxy)benzylidene]-2-[(5-nitrothiophen-2-yl) methylene]hydrazine ***7b***. Yellow powder. Yield: 143 mg (13%); mp 136–138 °C; R_f 0.82 (Hex : EtOAc 1 : 1, v/v). IR ν_{max} (cm^{-1}): 2921 (C–H), 1599 (C=N), 1547 (C=C), 1328 (N–O), 1158 (C–O); ^{1}H NMR (DMSO-d_6, 600 MHz) δ (ppm): 8.72 (s, 1H, H-1′), 8.52 (s, 1H, H-6), 8.16 (d, J = 4.4 Hz, 1H, H-4), 7.98 (d, J = 8.8 Hz, 2H, H-3′), 7.71 (d, J = 4.4 Hz, 1H, H-3), 7.49 (d, J = 7.5 Hz, 2H, H-8′), 7.42 (t, J = 7.5 Hz, 2H, H-9′), 7.36 (t, J = 7.5 Hz, 1H, H-10′), 7.26 (d, J = 8.8 Hz, 2H, H-4′), 5.24 (s, 2H, H-6′); ^{13}C NMR (DSMO-d_6, 151 MHz) δ (ppm): 162.9, 161.9, 155.5, 150.1, 136.6, 136.5, 133.0, 131.4, 129.1, 128.5, 128.0, 127.9, 125.8, 115.7, 69.6. HRMS-APCI (*pos*) m/z 366.0916 $[M + H]^+$ (Calcd. for $C_{19}H_{15}N_3O_3S^+$, 366.0912).

4-(E)-(E)-[(5-Nitrothiophen-2-yl)methylene] hydrazonomethylphenol ***8b***. Orange powder. Yield: 347 mg (42%); mp 243–245 °C; R_f 0.77 (hexane : EtOAc 1 : 1, v/v). IR ν_{max} (cm^{-1}): 3453 (O–H), 3089 (C–H), 1602 (C=N), 1492 (C=C), 1332 (N–O); ^{1}H NMR (DMSO-d_6, 600 MHz) δ (ppm): 10.22 (s, 1H, H-6′), 8.88 (s, 1H, H-1′), 8.63 (s, 1H, H-6), 8.17 (d, J = 4.4 Hz, 1H, H-4), 7.75 (d, J = 8.6 Hz, 2H, H-3′), 7.67 (d, J = 4.4 Hz, 1H, H-3), 6.88 (d, J = 8.6 Hz, 2H, H-4′); ^{13}C NMR (DMSO-d_6, 151 MHz) δ (ppm): 163.8, 161.3, 154.0, 151.9, 145.6, 131.8, 131.0, 130.4, 124.3, 116.0. HRMS-APCI (*pos*) m/z 276.0434 $[M + H]^+$ (Calcd. for $C_{12}H_9N_3O_3S^+$, 276.0443).

(1E,2E)-1-(4-Nitrobenzylidene)-2-[(5-nitrothiophen-2-yl) methylene]hydrazine ***9b***. Yellow powder. Yield: 303 mg (66%); mp 239–241 °C; R_f 0.53 (Hex : EtOAc 7 : 3, v/v). IR ν_{max} (cm^{-1}): 3108 (C–H), 1624 (C=N), 1595 (C=C), 1505 (N–O), 1336 (N–O); ^{1}H NMR (DMSO-d_6, 600 MHz) δ (ppm): 8.98 (s, 1H, H-1′), 8.87 (s, 1H, H-6), 8.35 (d, J = 8.7 Hz, 2H, H-4′), 8.19 (d, J = 4.3 Hz, 1H, H-4), 8.14 (d, J = 8.7 Hz, 2H, H-3′), 7.76 (d, J = 4.3 Hz, 1H, H-3); ^{13}C NMR (DMSO-d_6, 151 MHz) δ (ppm): 161.5, 156.5, 152.7, 149.1, 144.4, 139.2, 133.1, 130.3, 129.7, 124.1. HRMS-APCI (*pos*) m/z 305.0335 $[M + H]^+$ (Calcd. for $C_{12}H_8N_4O_4S^+$, 305.0345).

Azines 11 & 12. Furan-2-carboxaldehyde (furfural, 10) (3 mmol, 1 equiv.) was dissolved in anhydrous ethanol (10 mL) upon stirring and then substituted phenylhydrazone (3 mmol, 1 equiv.) and anhydrous potassium carbonate (6 mmol, 2 eq.) was added. The reaction mixture was stirred for 12 hours and monitored by TLC eluting with hexane : EtOAc (3 : 2, v/v). Upon completion, the reaction was quenched with water (50 mL), extracted with DCM (3 × 50 mL). The organic phase was dried over $MgSO_4$ and recrystallised from EtOAc to afford the desired azines.

(E)-1-[(E)-4-(Benzyloxy)benzylidene]-2-(furan-2-ylmethylene) hydrazine ***11***. Brown powder. Yield: 29%; mp 95–97 °C; R_f

0.72 (Hex : EtOAc 3 : 2, v/v). IR ν_{max} (cm^{-1}): 2924 (C–H), 1606 (C═N), 1509 (C═C), 1239 (C–O); ^{1}H NMR (DMSO-d_6, 600 MHz) δ (ppm): 8.64 (s, 1H, H-1′), 8.51 (s, 1H, H-6), 7.93 (s, 1H, H-5), 7.82 (d, J = 7.82 Hz, 2H, H-3′), 7.48 (d, J = 7.48 Hz, 2H, H-8′), 7.44 (t, J = 7.45 Hz, 1H, H-10′), 7.40 (d, J = 7.41 Hz, 2H, H-9′), 7.23 (d, J = 7.23 Hz, 1H, H-3), 7.15 (d, J = 7.14 Hz, 2H, H-4′), 6.97 (d, J = 6.96 Hz, 1H, H-4), 5.20 (s, 2H, H-6′); ^{13}C NMR (DMSO-d_6, 151 MHz) δ (ppm): 161.7, 161.4, 157.7, 150.2, 149.8, 146.8, 128.9, 128.4, 128.2, 128.0, 115.7, 114.9, 113.0, 69.9.

(E)-1-(Furan-2-ylmethylene)-2-[(E)-4-nitrobenzylidene] hydrazine ***12***. Yellow powder. Yield: 61%; mp 165–167 °C; R_f 0.66 (Hex : EtOAc 3 : 2, v/v). IR ν_{max} (cm^{-1}): 3122 (C–H), 1633 (C═N), 1593 (C═C), 1514 (N–O), 1278 (C–O); ^{1}H NMR (DMSO-d_6, 600 MHz) δ (ppm): 8.82 (s, 1H, H-1′), 8.59 (s, 1H, H-6), 8.34 (d, J = 8.34 Hz, 2H, H-4′), 8.12 (d, J = 8.12 Hz, 2H, H-3′), 7.99 (s, 1H, H-5), 7.21 (s, 1H, H-3), 6.75 (s, 1H, H-4); ^{13}C NMR (DMSO-d_6, 151 MHz) δ (ppm): 160.1, 152.0, 149.4, 147.6, 140.2, 129.8, 124.5, 118.8, 113.3.

The characterisation spectra of all derivatives are presented as ESI.†

Electrochemistry. In a typical experiment, a 0.5 mM solution of the ligand was dissolved in acetonitrile and 0.1 M NBu_4PF_6 (supporting electrolyte) and transfered to a three-electrode electrochemical cell (150 mL). Solutions were degassed with nitrogen for 5 minutes prior to each experiment. A platinum wire (Bio-Logic), Ag/AgCl electrode (Bio-Logic) and glassy carbon electrode (Bio-Logic) were used as counter, reference and working electrode, respectively. Before each experiment, the working electrode was polished with a 0.05 mm alumina suspension and subsequently washed with distilled water followed by acetonitrile. Cyclic voltammograms of the ligands were recorded at 25 °C in the range of −1.7 to 1.0 V using a scan rate of 100 mV s^{-1}, E step of 20 mV and scanned for 6 cycles each.

Biological evaluation

Leishmania antipromastigote assay. The antipromastigote activity of the synthesised compounds were evaluated according to Mangwegape *et al.*[68] The two *Leishmania* strains used were *Leishmania donovani* (strain 9515 (MHOM/IN/95/9515)) and *L. major* (strain IR-173 (MHOM/IR/-173)) promastigotes (BEI Resources, USA). They were cultured in Media 199 (M199) with Hank's salts, 0.68 mM L-glutamine, 4.2 mM sodium bicarbonate, 0.0001% biotin, 0.0005% hemin, 25 mM Hepes, 0.1 mM adenine (Sigma Aldrich), 10% fetal bovine serum (FBS; Thermofisher Scientific) and 50 U mL^{-1} penicillin/streptomycin (Pen/Strep) solution (Sigma Aldrich). The pH was adjusted to be between 7.3 and 7.4, and the promastigotes were maintained at 26 °C.

For the resazurin assay, 96 well plates (Nunc, Thermofisher Scientific) were seeded with 1.25×10^6 cells per mL (50 μL per well) logarithmic phase promastigotes with 50 μL of (i) 10 μM of compound for the screening of activity, or (ii) seven two-fold dilution concentrations of compounds for the determination of IC_{50} values. AmB (10 μM) served as the clinically available antileishmanial (standard) drug, and the blank consisted of growth medium without parasites. After incubation at 26 °C in humidified atmosphere for 48 hours, resazurin solution (50 μL of 0.01% in phosphate-buffered saline (PBS)) was added to and the plates were further incubated in the dark for 24 hours. A Thermofisher Scientific GO Multiscan plate reader was used to measure absorbance at both 570 nm and 600 nm. SkanIt 4.0 Research Edition software was used to perform data analysis for each biological replicate. Background absorbance of resazurin (600 nm) was subtracted from the absorbance values of resorufin (570 nm).

For the single-point activity screening, the following equation was used to determine growth inhibition percentage:

$$\text{Growth inhibition\%} = 100 - [(\Delta\text{Abs sample} - \Delta\text{Abs blank}) / (\Delta\text{Abs neg control} - \Delta\text{Abs blank}) \times 100]$$

Compounds with growth inhibition of >70% qualified for further IC_{50} evaluation.[69] To calculate the IC_{50}, cell viability was determined using the following equation:

$$\text{Cell viability\%} = (\Delta\text{Abs sample} - \Delta\text{Abs blank}) / (\Delta\text{Abs neg control} - \Delta\text{Abs blank}) \times 100$$

The IC_{50} and Z-score were determined for each compound's three biological replicates using the cell viability% values and GraphPad Prism 5. The final IC_{50} of each compound was determined by calculating the mean IC_{50}, with standard deviation of the biological replicates.

Intramacrophage antileishmanial assay. To evaluate the activity of the synthesised compounds against intramacrophage parasites, a modified method of Jain *et al.*[56] and Njanpa *et al.*[70] was used along with the two *Leishmania* strains used for the antipromastigote assay. Human monocytic leukemia (THP-1) cells (Cellonex, South Africa) were cultured in Roswell Park Memorial Institute (RPMI) 1640 medium with L-glutamine supplementation, 2 g L^{-1} sodium bicarbonate (Sigma Aldrich), 10% FBS (Thermofisher Scientific), and 1% Pen/Strep solution (Lonza). The cells were maintained in a humidified atmosphere at 37 °C and 5% CO_2.

A cell suspension of 500 000 cells per mL was prepared and 25 ng mL^{-1} phorbol 12-myristate 13-acetate (PMA) added before the addition of 200 μL per well to 96 well plates. The medium blank wells received only growth medium. The cells were incubated for 48 hours in a humidified atmosphere at 37 °C and 5% CO_2 to differentiate the suspension cell line to adherent macrophages. The plates were subsequently carefully washed with warmed PBS to remove non-differentiated cells. Stationary phase promastigotes were then added (200 μL per well) at a multiplicity of infection (MOI) of 30 : 1 in RPMI 1640 growth medium with 10% FBS. Parasite blank wells consisted of THP1 cells that did not receive

parasites. The plates were incubated for 24 hours at 32 °C, for IR173 strain, or 37 °C, for strain 9515, to promote infection. They were then carefully washed four times with warmed PBS to remove any remaining extracellular parasites with the wells then received 200 μL of growth medium with 10% FBS and compound: 10 μM for single-point activity screenings, seven three-fold dilution concentrations of 10 μM for IC_{50} determination, and 10 μM AmB for the standard drug control.

After 72 hours of incubation, the wells were again washed three times with warmed PBS to remove the FBS and any remaining extracellular promastigotes. The host macrophages were then lysed with 20 μL of 0.05% sodium dodecyl sulphate (SDS; Sigma Aldrich) in growth medium without FBS for 30 seconds, followed by the addition of 180 μL promastigote growth medium containing 10% FBS. For the resazurin assay, 10 μL of resazurin solution (0.25% in PBS) was added to each well and the plates were further incubated at 26 °C for 72 hours in the dark to accommodate parasite recovery to promastigote forms. Absorbance measurements and data analysis were performed exactly as described for the antipromastigote assay. With regards to the activity screening, compounds with a growth inhibition of >60% qualified for further IC_{50} determination.[55]

***T. cruzi* anti-epimastigote assay.** To evaluate the anti-epimastigote activity of the synthesised compounds, the resazurin assay used for the *Leishmania* antipromastigote activity was applied, with modifications to only the growth conditions and parasite seeding density used.

T. cruzi strain CL (BEI Resources, USA) was cultured in LIT medium, consisting of 5 mg mL^{-1} Bacto™ tryptose (BD Biosciences), 9 mg mL^{-1} Difco™ liver infusion broth (BD Biosciences), 8 mg mL^{-1} Na_2HPO_4, 1 mg mL^{-1} NaCl, 0.4 mg mL^{-1} KCl, 1 mg mL^{-1} glucose, 10% FBS and 0.01 mg mL^{-1} hemin (Sigma Aldrich), pH 7.2. The epimastigotes were maintained at 25 °C. For the resazurin assay, epimastigotes (5×10^5 cells per well, final volume 100 μL per well) were seeded in 96 well plates (Nunc, Thermofisher Scientific) in the presence of compounds and blanks as described for the antipromastigote assay. The plates were then incubated at 25 °C in humidified atmosphere for 48 hours, followed by the addition of 50 μL of resazurin solution and 24-hour incubation. Absorbance and data analysis were performed for each biological replicate as indicated for the *Leishmania* antipromastigote assay.

With regards to the activity screening, there are currently no reports of cut-off growth inhibition values for anti-epimastigote activity. As the epimastigotes are cultured and assayed similarly to *Leishmania* promastigotes, the growth inhibition cut-off of >70% was also applied for qualifying compounds for IC_{50} determination.

***T. cruzi* antitrypomastigote assay.** The activity of compounds against extracellular bloodstream forms (trypomastigotes) of *T. cruzi* were evaluated using an adapted method of de Freitas Oliveira *et al.*[69]

Cultured epimastigotes were centrifuged and resuspended in minimal essential medium (MEM) supplemented with 3% FBS for addition to a monolayer of cultured African green monkey kidney (Vero) cells (Cellonex, South Africa), which were maintained as indicated in the following cytotoxicity section. By changing the Vero culture media to MEM, the growth rate of the Vero cells is reduced, which in turn prevents reduced infection due to host cell proliferation. The co-culture was then maintained for 5–15 days until sufficient trypomastigotes formed.

The growth medium of the flask was collected and centrifuged at 3000 × *g* for 10 min, the supernatant discarded and replaced with fresh growth medium with 10% FBS. The parasites were counted using a hemocytometer and the cell density adjusted to 1×10^7 cells per mL and >80% trypomastigote forms. The trypomastigotes were then seeded in 96 well plates (200 μL per well) in the presence of compounds and blanks as described for the antipromastigote assay. Benznidazole (10 μM) was used as standard drug. The plates were incubated for 48 hours in humidified atmosphere at 37 °C and 5% CO_2, followed by the addition of 50 μL of resazurin solution and 24-hour incubation. Absorbance and data analysis were performed for each biological replicate as indicated for the *Leishmania* antipromastigote assay.

With regards to the activity screening, there are currently no reports of cut-off growth inhibition values for *T. cruzi* anti-trypomastigote activity. Due to the axenic/host-free nature of the trypomastigote cultures, a cut-off of >70% was selected.

Cytotoxicity assays

General/basal cytotoxicity. The general cytotoxicity of synthesised compounds was evaluated using Vero cells and the resazurin assay.[71]

Vero cells were maintained in Hyclone Dulbecco's modified Eagle's medium, with high glucose (separations), 10% FBS and 1% L-glutamine, Pen/Strep, and non-essential amino acids, in a humidified atmosphere at 37 °C and 5% CO_2. For the resazurin assay, 96 well plates with 100 μL of cell suspension (60 000 cells per mL) were prepared and incubated for 24 hours. The cells were then treated with seven two-fold dilutions of 100 μM compound in growth medium. Emetine dihydrochloride (1 μM) served as positive control and the blanks contained growth medium without cells. The treated plates were then incubated for 48 hours and the resazurin assay initiated *via* the addition of 50 μL of resazurin solution and further incubation for 2 hours. Absorbance and data analysis were performed for each biological replicate as described for the *Leishmania* antipromastigote assay.

Host macrophage cytotoxicity. Duplicate 96 well plates of differentiated THP1 cells were prepared during the host cell preparations of the intramacrophage antileishmanial assay. After 72 hours of PMA treatment, the growth medium was removed, and the wells treated with seven three-fold dilution of 100 μM of compounds that qualifies for IC_{50}

determination. The plates were then incubated for 72 hours in a humidified atmosphere at 37 °C and 5% CO_2, followed by the addition of 50 μL of resazurin solution and 3-hour incubation. Absorbance and data analysis were performed for each biological replicate as indicated for the *Leishmania* antipromastigote assay.

Statistical analysis

In vitro antileishmanial and antitrypanosomal activities and cytotoxicity (indicated as IC_{50} values), were derived from non-linear regression analysis. Results were represented as the mean ± the standard deviation (SD) from the triplicate biological experiments. Statistical analysis was performed using SkanIt 4.0 Research Edition software (Thermofisher Scientific) and Prism V5 software (GraphPad). All reported data is significant at $p < 0.05$.

Disclaimer

Any opinions, findings, conclusions, and/or recommendations expressed in this material are those of the authors and therefore the NRF does not accept any liability in this regard.

Ethics

Ethics approval for this study was obtained from the Human Research Ethics Committee of the North-West University (NWU-00385-20-A1).

Abbreviations

NTDs	Neglected tropical diseases
CL	Cutaneous leishmaniasis
MCL	Mucocutaneous leishmaniasis
VL	Visceral leishmaniasis
cNFs	Clinical nitrofurans
ROS	Reactive oxygen species
NFA	5-Nitro-2-furaldehyde
NTA	5-Nitrothiophene-2-carboxaldehyde
NFX	Nifuroxazide
NTX	Nifurtimox
FZD	Furazolidone
NFZ	Nitrofurazone
NFT	Nitrofurantoin
AmB	Amphotericin B
Em	Emetine
WHO	World Health Organization

Author contributions

Conceptualisation: [David D. N'Da]; methodology: [Maryna Saayman, Christina Kannigadu, Janine Aucamp, Cassiem Joseph, Andrew J. Swarts, David D. N'Da]; formal analysis and investigation: [Maryna Saayman, Janine Aucamp, Helena D. Janse van Rensburg, Christina Kannigadu, David D. N'Da]; writing – original draft preparation: [Maryna Saayman, Christina Kannigadu, Janine Aucamp]; writing – review and editing: [Christina Kannigadu, Janine Aucamp, Cassiem Joseph, Andrew J. Swarts, David D. N'Da]; funding acquisition: [David D. N'Da]; resources: [David D. N'Da]; supervision: [David D. N'Da].

Conflicts of interest

The authors have no conflicts to declare.

Acknowledgements

This work was financially supported by the South African National Research Foundation (NRF) (UID 129324 and 148781) and the North-West University. The following reagents were obtained through BEI Resources, NIAID, NIH: *Leishmania donovani*, Strain 9515 (MHOM/IN/95/9515), NR-48822, *Leishmania major*, Strain IR173 (MHOM/IR/-173), NR-48816, *Trypanosoma cruzi*, Strain CL, NR-49381.

References

1 WHO, Neglected Tropical Diseases: Overview, 2023, **https://www.who.int/health-topics/neglected-tropical-diseases#tab=tab_1**, [Date of access: March 2023].
2 WHO, Neglected tropical diseases: Impact, 2023, **https://www.who.int/health-topics/neglected-tropical-diseases#tab=tab_2**, [Date of access: March 2023].
3 M. P. Barrett and S. L. Croft, *Br. Med. Bull.*, 2012, **104**, 175–196.
4 WHO, Leishmaniasis: Overview, 2023, **https://www.who.int/health-topics/leishmaniasis#tab=tab_1**, [Date of access: March 2023].
5 N. Salam, W. M. Al-Shaqha and A. Azzi, *PLoS Neglected Trop. Dis.*, 2014, **8**, e3208.
6 E. Torres-Guerrero, M. R. Quintanilla-Cedillo, J. Ruiz-Esmenjaud and R. Arenas, *F1000Research*, 2017, **6**, 750.
7 WHO, Leishmaniasis: Key facts, 2023, **https://www.who.int/news-room/fact-sheets/detail/leishmaniasis**, [Date of access: March 2023].
8 WHO, Number of cases of cutaneous leishmaniasis reported, 2023, **https://www.who.int/data/gho/data/indicators/indicator-details/GHO/number-of-cases-of-cutaneous-leishmaniasis-reported**, [Date of access: March 2023].
9 WHO, Number of cases of cutaneous leishmaniasis reported, 2023, **https://www.who.int/data/gho/data/indicators/indicator-details/GHO/number-of-cases-of-cutaneous-leishmaniasis-reported**, [Date of access: March 2023].
10 WHO, Report of WHO Expert Committee on the Control of Leishmaniases, Geneva: World Health Organization, 2010, **https://apps.who.int/iris/handle/10665/44412**, [Date of access: March 2023].
11 WHO, Chagas disease: Key facts, 2022, **https://www.who.int/news-room/fact-sheets/detail/chagas-disease-(american-trypanosomiasis)**, [Date of access: March 2023].

12 WHO, Chagas disease (American trypanosomiasis): Overview, 2023, **https://www.who.int/health-topics/chagas-disease#tab=tab_1**, [Date of access: March 2023].
13 E. Chatelain, *Comput. Struct. Biotechnol. J.*, 2017, **15**, 98–103.
14 D. A. Álvarez-Hernández, G. A. Franyuti-Kelly, R. Díaz-López-Silva, A. M. González-Chávez, D. González-Hermosillo-Cornejo and R. Vázquez-López, *Rev. Med. Hosp. Gen.*, 2018, **81**, 154–164.
15 PAHO, Chagas disease, 2023, **https://www.paho.org/en/topics/chagas-disease**, [Date of access: March 2023].
16 S. P. Georgiadou, K. P. Makaritsis and G. N. Dalekos, *J. Transl. Int. Med.*, 2015, **3**, 43–50.
17 M. Ghorbani and R. Farhoudi, *Drug Des., Dev. Ther.*, 2018, **12**, 25–40.
18 S. S. Braga, *Eur. J. Med. Chem.*, 2019, **183**, 111660.
19 L. H. Freitas-Junior, E. Chatelain, H. A. Kim and J. L. Siqueira-Neto, *Int. J. Parasitol.: Drugs Drug Resist.*, 2012, **2**, 11–19.
20 H. C. Maltezou, *J. Biomed. Biotechnol.*, 2010, **2010**, 617521.
21 S. J. Martinez, P. S. Romano and D. M. Engman, *Front. Cell. Infect. Microbiol.*, 2020, **10**, 1–11.
22 WHO, Chagas disease (American trypanosomiasis): Treatment, 2023, **https://www.who.int/health-topics/chagas-disease#tab=tab_3**, [Date of access: March 2023].
23 R. Patel, L. Rinker, J. Peng and W. M. Chilian, in *Reactive Oxygen Species (ROS) in Living Cells*, ed. C. Filip and E. Albu, IntechOpen, London, 2018, pp. 7–20.
24 N. H. Zuma, J. Aucamp and D. D. N'Da, *Eur. J. Pharm. Sci.*, 2019, **140**, 105092.
25 C. Pal and U. Bandyopadhyay, *Antioxid. Redox Signaling*, 2012, **17**, 555–582.
26 R. Sreenivasulu, K. T. Reddy, P. Sujitha, C. G. Kumar and R. R. Raju, *Bioorg. Med. Chem.*, 2019, **27**, 1043–1055.
27 V. Manikandan, S. Balaji, R. Senbagam, R. Vijayakumar, M. Rajarajan, G. Vanangamudi, R. Arulkumaran, R. Sundararajan and G. Thirunarayanan, *Int. J. Adv. Chem.*, 2017, **5**, 17–24.
28 B. Glinma, F. A. Gbaguidi, U. C. Kasséhin, S. D. S. Kpoviessi, A. Houngbèmè, H. D. Houngue, G. C. Accrombessi and J. H. Poupaert, *J. Appl. Pharm. Sci.*, 2015, **5**, 001–007.
29 V. T. Angelova, V. Valcheva, N. G. Vassilev, R. Buyukliev, G. Momekov, I. Dimitrov, L. Saso, M. Djukic and B. Shivachev, *Bioorg. Med. Chem. Lett.*, 2017, **27**, 223–227.
30 L. Dehestani, N. Ahangar, S. M. Hashemi, H. Irannejad, P. Honarchian Masihi, A. Shakiba and S. Emami, *Bioorg. Chem.*, 2018, **78**, 119–129.
31 A. Kajal, S. Bala, N. Sharma, S. Kamboj and V. Saini, *Int. J. Med. Chem.*, 2014, **2014**, 761030.
32 L. Navidpour, H. Shafaroodi, G. Saeedi-Motahar and A. Shafiee, *Med. Chem. Res.*, 2014, **23**, 2793–2802.
33 S. S. Chourasiya, D. Kathuria, A. A. Wani and P. V. Bharatam, *Org. Biomol. Chem.*, 2019, **17**, 8486–8521.
34 B. Singh and A. Pandey, *Liq. Cryst.*, 2009, **37**, 57–67.
35 J. Gómez, A. H. Klahn, M. Fuentealba, D. Sierra, C. Olea-Azar, J. D. Maya and M. E. Medina, *J. Organomet. Chem.*, 2017, **839**, 108–115.
36 S. E. Ward and P. Beswick, *Expert Opin. Drug Discovery*, 2014, **9**, 995–1003.
37 C. J. Abelt and J. M. Pleier, *J. Am. Chem. Soc.*, 1989, **111**, 1795–1799.
38 I. Alkorta, F. Blanco and J. Elguero, *ARKIVOC*, 2007, **2008**, 48–56.
39 N. P. Neureiter, *J. Am. Chem. Soc.*, 1959, **81**, 2910.
40 R. Karmakar, C. R. Choudhury, S. R. Batten and S. Mitra, *J. Mol. Struct.*, 2007, **826**, 75–81.
41 J. Gómez, A. Hugo Klahn, M. Fuentealba, D. Sierra, C. Olea-Azar and M. E. Medina, *Inorg. Chem. Commun.*, 2015, **61**, 204–206.
42 C. W. Lindsley, in *Encyclopedia of Psychopharmacology*, ed. I. Stolerman and L. Price, Springer Berlin Heidelberg, Berlin, Heidelberg, 2014, pp. 1–6, DOI: **10.1007/978-3-642-27772-6_7015-1**.
43 A. K. Ghose, V. N. Viswanadhan and J. J. Wendoloski, *J. Phys. Chem. A*, 1998, **102**, 3762–3772.
44 C. Lipinski, F. Lombardo, B. W. Dominy and P. J. Feeney, *Adv. Drug Delivery Rev.*, 2001, **46**, 3–26.
45 J. A. Arnott and S. L. Planey, *Expert Opin. Drug Discovery*, 2012, **7**, 863–875.
46 G. Caron and G. Ermondi, *Future Med. Chem.*, 2016, **8**, 2013–2016.
47 T. Reinhardt, K. M. Lee, L. Niederegger, C. R. Hess and S. A. Sieber, *ACS Chem. Biol.*, 2022, **17**, 3077–3085.
48 J. H. Tocher, *Gen. Pharmacol.*, 1997, **28**, 485–487.
49 S. J. Teague, A. M. Davis, P. D. Leeson and T. Oprea, *Angew. Chem., Int. Ed.*, 1999, **38**, 3743–3748.
50 B. S. McGwire and A. R. Satoskar, *QJM*, 2014, **107**, 7–14.
51 CDC, American Trypanosomiasis, 2021, **https://www.cdc.gov/dpdx/trypanosomiasisamerican/index.html**, [Date of access: March 2023].
52 K. Katsuno, J. N. Burrows, K. Duncan, R. Hooft van Huijsduijnen, T. Kaneko, K. Kita, C. E. Mowbray, D. Schmatz, P. Warner and B. T. Slingsby, *Nat. Rev. Drug Discovery*, 2015, **14**, 751–758.
53 F. Villalta and G. Rachakonda, *Expert Opin. Drug Discovery*, 2019, **14**, 1161–1174.
54 J. L. Siqueira-Neto, O.-R. Song, H. Oh, J.-H. Sohn, G. Yang, J. Nam, J. Jang, J. Cechetto, C. B. Lee, S. Moon, A. Genovesio, E. Chatelain, T. Christophe and L. H. Freitas-Junior, *PLoS Neglected Trop. Dis.*, 2010, **4**, e675.
55 G. De Muylder, K. K. H. Ang, S. Chen, M. R. Arkin, J. C. Engel and J. H. McKerrow, *PLoS Neglected Trop. Dis.*, 2011, **5**, e1253.
56 S. K. Jain, R. Sahu, L. A. Walker and B. L. Tekwani, *J. Visualized Exp.*, 2012, **70**, 4054.
57 N. S. Finiuk, V. P. Hreniuh, Y. V. Ostapiuk, V. S. Matiychuk, D. A. Frolov, M. D. Obushak, R. S. Stoika and A. M. Babsky, *Biopolym. Cell*, 2017, **33**, 135–146.
58 S. Liu, M. Su, S. J. Song and J. H. Jung, *Mar. Drugs*, 2017, **15**, 329.
59 J. Fu, H. Chen, D. N. Soroka, R. F. Warin and S. Sang, *J. Agric. Food Chem.*, 2014, **62**, 4632–4642.
60 E. A. Adewusi, P. Steenkamp, G. Fouche and V. Steenkamp, *Nat. Prod. Commun.*, 2013, **8**, 1213–1216.

61 R. Lira, S. Sundar, A. Makharia, R. Kenney, A. Gam, E. Saraiva and D. Sacks, *J. Infect. Dis.*, 1999, **180**, 564–567.
62 J. E. Potvin, P. Leprohon, M. Queffeulou, S. Sundar and M. Ouellette, *Clin. Infect. Dis.*, 2021, **72**, e526–e532.
63 C. A. Bauer, G. Schneider and A. H. Göller, *J. Cheminform.*, 2019, **11**, 59.
64 G. Papadatos and N. Brown, *WIREs Comput. Mol. Sci.*, 2013, **3**, 339–354.
65 N. A. Meanwell, *J. Med. Chem.*, 2011, **54**, 2529–2591.
66 A. Firth and P. Prathapan, *Curr. Res. Pharmacol. Drug Discov.*, 2021, **2**, 100011.
67 J. Aucamp and D. D. N'Da, *Exp. Parasitol.*, 2022, **236–237**, 108249.
68 D. K. Mangwegape, N. H. Zuma, J. Aucamp and D. D. N'Da, *Arch. Pharm.*, 2021, **354**, e2000280.
69 J. W. de Freitas Oliveira, T. M. Torres, C. J. G. Moreno, B. Amorim-Carmo, I. Z. Damasceno, A. K. M. C. Soares, J. da Silva Barbosa, H. A. O. Rocha and M. S. Silva, *Sci. Rep.*, 2021, **11**, 11200.
70 C. A. N. Njanpa, S. C. N. Wouamba, L. R. T. Yamthe, D. Dize, B. M. T. Tchatat, P. V. F. Tsouh, M. N. Pouofo, J. B. Jouda, B. L. Ndjakou, N. Sewald, S. F. Kouam and F. F. Boyom, *BMC Complementary Med. Ther.*, 2021, **21**, 106.
71 E. M. Czekanska, *Methods Mol. Biol.*, 2011, **740**, 27–32.